



Cite this: *Green Chem.*, 2022, **24**, 1895

## Status and advances of deep eutectic solvents for metal separation and recovery

Ziwen Yuan,<sup>a</sup> Hang Liu,<sup>b</sup> Wai Fen Yong,<sup>c,d</sup> Qianhong She<sup>id \*a,e</sup> and Jesús Esteban<sup>id \*f</sup>

The increasing discharge of metal-associated waste not only causes growing concerns on the environment and human health but also accelerates the depletion of natural metal resources. Within this context and driven by circular economy, metal recovery is a topic of increasing research interest. Solvent extraction and leaching are commonly the major processes for metal separation and recovery from various resources. Conventional solvents used in these processes often exhibit aggressive profiles that may lead to health, environment and safety related issues as well as damage to industrial equipment. With the aim to make these separation processes safer and cleaner, it is necessary to explore the use of greener solvents. Deep eutectic solvents (DESSs), a family of neoteric solvents, have emerged and attracted increasing interest in the last few years. DESSs have been regarded as a type of interesting alternative to ionic liquids (ILs) owing to their ease of preparation, high biodegradability, low toxicity and high tunability. Lately, their use has started being reported for metal recovery and separation from matrices like electronic waste, minerals, biological samples, environmental samples such as soil and wastewater, food and cosmetics. This review covers a description of DESSs and their properties together with the fundamentals of their use as an alternative medium to conduct metal separation from different sources. Finally, a literature survey of their application in metal detection, separation and recovery, in recent works is presented.

Received 17th October 2021,  
Accepted 17th February 2022

DOI: 10.1039/d1gc03851f

[rsc.li/greenchem](http://rsc.li/greenchem)

### 1. Introduction

With the rapid development of global economy and the increase in world population, the demand for metals is continuously increasing. Due to the finite resources, many countries worldwide are facing metal scarcity within their exploitable reserves. This can lead to an endangerment of the present way of life and economic development in general, particularly considering the growing amounts of electronic devices present in different activities. The current market value of some metals makes it of paramount importance to devise strategies to recover them, examples of which are Au (USD 1859 per ounce), Pd (USD 2761 per ounce), Pt (USD

1151 per ounce), Ag (USD 27.7 per ounce) or Rh (EUR 73 320 per kg).<sup>1</sup>

Further to this point, by way of an example, in China the annual demands for Pt and Pd amounted to more than 141 tons, however, only less than 3 tons of platinum group metals were mined with total reserve of only about 350 tons.<sup>2</sup> Co, Mg, In, rare earth elements, platinum group metals and others were listed as critical raw materials by the European Commission due to their supply risk and economic importance.<sup>3</sup> In contrast with the increasingly severe metal scarcity, there is a substantial amount of metal present in the waste from industry and daily life. To tackle the issue of metal scarcity, extensive efforts have been dedicated to exploring alternative sources of metals and recovery from these sources would not only create substantial economic benefits, but also alleviate the threat of these metals especially heavy metals on human health and environment. Waste is increasingly becoming a major resource within the context of circular economy and the strategy of recovering metals falls within the remit of the United Nations Sustainable Development Goals (SDGs), particularly SDG12 (sustainable production and consumption). Also, considering the potential subsequent impact on the environment, it also aligns with SDG3 (good health and well-being), SDG14 (life below water) and SDG15 (life on land).<sup>4</sup>

<sup>a</sup>School of Civil and Environmental Engineering, Nanyang Technological University, Singapore 639798. E-mail: qhshe@ntu.edu.sg

<sup>b</sup>Key Laboratory of Drinking Water Science and Technology, Research Center for Eco-Environmental Sciences, Chinese Academy of Sciences, China

<sup>c</sup>School of Energy and Chemical Engineering, Xiamen University Malaysia, Selangor Darul Ehsan 43900, Malaysia

<sup>d</sup>College of Chemistry and Chemical Engineering, Xiamen University, Xiamen 361005, Fujian, China

<sup>e</sup>Singapore Membrane Technology Centre, Nanyang Environment & Water Research Institute, Nanyang Technological University, Singapore 637141

<sup>f</sup>Department of Chemical Engineering, The University of Manchester, Manchester M13 9PL, UK. E-mail: [jesus.estebanserrano@manchester.ac.uk](mailto:jesus.estebanserrano@manchester.ac.uk)



Metals can be recovered from a number of unconventional sources. These include recycling industrial waste, which on occasions can have a high content and purity of metals, such as zinc oxide dust containing large amount of Zn, Pb and Cu<sup>5</sup> or spent catalysts.<sup>6,7</sup> Very significantly, another source that is attracting increasing attention over the last years is waste electrical and electronic equipment, also widely known as e-waste, among which are spent lithium-ion batteries (LIBs) as a relevant case. It is estimated that approximately 42% of this class of waste originates from household appliances, followed by 34% of communication devices, 14% of other electronic items and the remaining 10% from different accessories<sup>8</sup> and that 3–4% wt of it consists in precious metals.<sup>9</sup>

As recently as in 2019, the amount of e-waste generated reached 53.6 Mton with an estimation of sustained growth at an annual rate of about 2 Mton given the widespread use of electronic equipment. By continents, the most significant producer is Asia with a total 24.9 Mton, of which the major producers were China with 10.1 Mton, India with 3.23 Mton, Japan with 2.57 Mton and Indonesia with 1.62 Mton. The following major producers globally are the USA with 13.1 Mton and Europe with 12 Mton.<sup>10,11</sup> The work by Nithya *et al.* (2021)<sup>11</sup> not only highlighted the magnitude of the issue raised by Forti *et al.* (2020),<sup>10</sup> but also the need to adopt global and regional policies to properly address proper recycling technologies as in many cases e-waste is treated simply as domestic waste. In these regards, recycling was performed formally only for 9.3 Mton (17.4%) of the total e-waste generation of 2019, with the remainder being left untreated. Although still poor, the figures in 2019 represented a significant improvement with respect to the 1.8 Mton recycled in 2014. Europe made the highest efforts in this case treating 42.5% of the waste, followed by Asia with 11.7%, whereas the rest of the continents still fall below 10%.<sup>10,11</sup>

Metal recovery can be undertaken with a series of technologies. The so-called informal recycling refers to practices with no consideration towards environmental, health and safety

(EHS) concerns in any form. One way to do this is the indiscriminate open combustion to recover metals like Cu, Al, Au, Pb, Hg, Cd, Pd or Pt, which entails serious consequences to the environment. To recover some of the mentioned metals, sometimes strong acids like hydrochloric acid (HCl), nitric acid (HNO<sub>3</sub>), or sulfuric acid (H<sub>2</sub>SO<sub>4</sub>) are used.<sup>11</sup>

Other routes for the formal recycling of metals have been explored not just for the sake of environmental concerns but also because they can be more efficient. Considering the heterogeneous composition of the components of e-waste and printed circuit boards, these processes typically start with physical pretreatments to segregate the non-metallic and metallic fractions. The metallic fraction can then undergo further processes, among which are pyrometallurgy, hydrometallurgy or biometallurgy.<sup>11–14</sup>

Pyrometallurgy is the most conventional treatment used despite its high energy intensive nature. To separate Cu, Au and Ag, most e-waste is treated in smelters going through a blast furnace. Then, it undergoes upgrading in an anode furnace and is then refined by electrolysis or the so-called electrowinning for metal recovery. Industrial examples of pyrometallurgical metal recovery processes include the Noranda process in Canada, Ronnskar in Sweden, Umicore in Belgium and Aurubis in Germany. However, this process originates severe emissions including slag, soot, flue gases and other toxic pollutants.<sup>11–13,15</sup>

Hydrometallurgy offers better possibilities for control and reliability in addition to being less environmentally harmful. The process involves leaching of the metals by acid or caustic treatment. Chemical leaching was originally performed with cyanide, although this option has been disregarded for obvious toxicity reasons. Other options involve the use of strong inorganic acids, which can lead to high corrosiveness. More recently, less aggressive treatments with thiourea or thio-sulfate as well as leaching with ligands, etching, bioleaching or ILs have been proposed. The leachate can then undergo subsequent purification techniques, among which are electro-



Ziwen Yuan

Ziwen Yuan obtained his PhD degree in Chemical Engineering in 2021 from The University of Sydney in Australia. Then he joined Nanyang Technological University (NTU) in Singapore as a research fellow. His research focuses on the development of sustainable and environmentally friendly membrane-based technologies for water treatment, purification, desalination, and resource recovery (such as low-grade waste heat, metals, etc.).



Hang Liu

Hang Liu is an Assistant Professor at the Research Center for Eco-Environmental Sciences (RCEES), Chinese Academy of Sciences. Prior to starting at RCEES, Hang Liu received her Ph.D. in Environmental Sciences from Tianjin University in 2018, and was a visiting Ph.D. student and postdoctoral researcher at Nanyang Environment & Water Research Institute, Nanyang Technological University from 2015 to 2019. Her research focuses on hybrid processes for water and wastewater treatment.



deposition, ion exchange, adsorption and, also, solvent extraction, for which the search for new solvents is always relevant.<sup>11–13,15</sup>

Biometallurgy has become yet another strategy for metal recovery that has the advantages of low costs and energy consumption, although the kinetics of the process is somewhat limiting. Bioleaching takes place first, for which acidophilic bacteria like *Acidithiobacillus ferroxidans*, *A. thiooxidans* or *Sulfolobus* sp. are used, which oxidize ferrous ions and reduce sulfur compounds and are capable of solubilizing metals like Cu, Zn, Al or Ni. Then, biosorption occurs, which involves phenomena like complexation, ion exchange, chelation or coordination involving microorganisms that include fungi, algae or yeasts.<sup>12,16,17</sup>

Other than the three main methods mentioned above, other techniques are slowly gaining momentum, such as the use of supercritical CO<sub>2</sub>, cryomilling, different chelation technologies or employing ILs.<sup>12,18</sup>

In addition to the obvious economic impact of recovering metals from waste sources, as addressed before, metal removal and separation can be a very important aspect for human health and safety as well as environmental aspects. A good deal of work has been dedicated to metal removal for the remediation of wastewater.<sup>19</sup> For instance, heavy metals can be present in drinking water bodies and their consumption should be avoided even in trace amounts.<sup>20</sup> Another case would be the presence of cadmium in pigments in cosmetics and beauty products such as lipstick. In contact with human tissues, it could be absorbed and lead to undesired bioaccumulation.<sup>21,22</sup> Here methods for extraction include liquid-based extractions (aqueous biphasic systems, three-liquid-phase extraction, cloud point extraction or liquid membrane extractions), solid phase extractions (using nanosorbent, polymeric or magnetic materials, metal organic frameworks,

ion exchange or solid-phase microextractions) or bulk sorbent methods (chemical precipitation, or biosorbent extraction).<sup>23</sup> In this sort of treatments and technologies for metal separation, it is important to utilize solvents that show low toxicity and high biodegradability.

The search for safer solvents for a more sustainable chemical practice is of paramount importance and has received much attention in the last years.<sup>24–27</sup> Whilst ionic liquids (ILs) have been used for metal separation processes,<sup>28,29</sup> deep eutectic solvents (DESSs) are neoteric solvents that appear as a very interesting alternative considering their advantages, including their low cost and high tunability.<sup>30–32</sup> In the last years, the use of DESSs has attracted a growing interest in research. Compared with the conventional organic solvents, DESSs inherit the advantages of ILs of good thermal and chemical stability, designable properties by varying compositions, environmentally friendly with low vapor pressure and difficult volatilization,<sup>33</sup> while it further exhibits some favorable features such as more convenient preparation methods, higher purity of synthetic products, lower cost, less corrosive effects on the equipment, relatively easier biodegradation (especially for the vast majority generated with choline chloride (ChCl)) and generally lower toxicity. As for the latter aspect, it is important to remark that despite DESSs having favourable EHS profiles, these have to be evaluated on a one-by-one basis as some of the individual components of which they are made can be harmful. One example could be the DES prepared from ChCl and ethylene glycol, the latter of which is known to be toxic to humans.

Apart from other applications, their use in separation processes has been prominent in the last years. Fig. 1a and b show a comparison of the number of publications and citations, respectively, of references that include in their titles the terms “eutectic solvent” and either “recovery”, “extraction” or “separation”, being the latter three mutually exclusive. The



**Wai Fen Yong**

*Wai Fen Yong is an Associate Professor of School of Energy and Chemical Engineering, Xiamen University Malaysia. She obtained her PhD degree in Chemical and Biomolecular Engineering from National University of Singapore (NUS). Her research focuses on developing sustainable materials and membrane technologies for biogas separation, industrial air purification and water purification. She was awarded as*

*Chartered Engineer by IChemE, UK in 2019. She won prestigious awards including 2016 Green Talents Award and Top 50 outstanding Green Talents alumni from the German Federal Ministry of Education and Research (BMBF) and Finalist of the Energy and Sustainability Awards from IChemE, Singapore.*



**Qianhong She**

*Qianhong She is an Assistant Professor in the School of Civil and Environmental Engineering at Nanyang Technological University (NTU) in Singapore. Prior to the current position, he was a Lecturer in the School of Chemical and Biomolecular Engineering at The University of Sydney in Australia from 2017–2019. His research is on the development of various separation technologies to tackle pressing environmental issues,*

*produce clean water via desalination and wastewater reclamation, separate chemical/biological products, and transform waste into value-added materials and/or clean energy. He received the Green Talents Award from the German Federal Ministry of Education and Research (BMBF) in 2016.*



same search procedure was performed for “ionic liquid”. As can be seen for the case of eutectic solvents, from the first references dating from 2013, there has been a substantial and sustained increase both in publications and citations up to the present date. In the case of ionic liquids, the first references and citations date from slightly before 2000. Whilst the citations have understandably continued to grow up to this date, it can be seen that the trend in the number of publications with ionic liquids has shifted and less works have been released from 2017 onwards. Remarkably, the increase in the number of publications for eutectic solvents in their first few years is more significant than that of ionic liquids. As for the recovery of metals, this topic has been studied for several decades now, but it has only been again since approximately 2012 that researchers have paid more attention to this issue. For reference, Fig. 1c and d show the number of publications and citations from 2000 to the present date featuring the terms “metal recovery”, “metal extraction” or “metal separation” in their titles.

In view of the relevance of metal recovery for resource conservation and the increasing interest in the use of DESs as a cleaner alternative to perform the relevant separations, here we present an account of this emerging field. In the following, an overview of deep eutectic solvents is presented together with what properties and mechanisms are relevant for metal extraction. Finally, a survey of the works published recently in literature is given to exemplify the prospects of this technology.

Two commonly used parameters (*i.e.*, distribution ratio  $D$  and percentage extraction % $E$ ) of the performance of metal

recovery and separation processes are calculated using following equations:

Distribution ratio ( $D$ ) is defined by the total concentration of a metal Me (sum of all forms) expressed as either total mass of metal atoms or radioactivity per liter in the organic phase divided by the total of the metal (sum of all forms) in the aqueous layer, which can be written as:<sup>34</sup>

$$D_{\text{Me}} = \frac{[\text{Me}]_{\text{t,org}}}{[\text{Me}]_{\text{t,aq}}}$$

when Me is present in various complex forms in the aqueous phase and in the organic phase,  $[\text{Me}]_{\text{t}}$  refers to the sum of the mass concentrations of all forms of Me in the given phase. The subscript “t” indicates total Me (sum of all forms), whereas org and aq refer to the organic phase and aqueous phase, respectively.

Note that another commonly used parameter, partition coefficient ( $K_{\text{d}}$ ), is easily confused with distribution ratio ( $D$ ).  $K_{\text{d}}$  is defined as the concentration of a specific species in the organic phase divided by its concentration in the aqueous phase:

$$K_{\text{d,A}} = \frac{[\text{A}]_{\text{org}}}{[\text{A}]_{\text{aq}}}$$

where  $[\text{A}]$  refers to the concentration of a species A in the given phase.

An example is given here to further explain the difference between the distribution ratio  $D$  and the partition coefficient  $K_{\text{d}}$ : a liquid–liquid extraction process in which a hydrated metal such as  $[\text{Am}(\text{H}_2\text{O})_n]^{3+}$  is in equilibrium with a lipophilic (hydrophobic) complex  $\text{AmL}_3$ . If the aqueous phase contains 10 picomoles per liter of americium as  $\text{AmL}_3$  and 90 picomoles per liter of hydrated americium ( $[\text{Am}(\text{H}_2\text{O})_n]^{3+}$ ), and the organic layer contains 10 000 picomoles per liter of  $\text{AmL}_3$ , the  $D$  of the americium is 100, while the  $K_{\text{d}}$  values for  $[\text{Am}(\text{H}_2\text{O})_n]^{3+}$  and  $\text{AmL}_3$  are zero and 1000 respectively.

In terms of percentage extraction (% $E$ , or known as extraction efficiency), it is defined as the percentage of the total amount of target substance in all extractants with respect to that in the initial source, which can be expressed as:<sup>35,36</sup>

$$\begin{aligned} \%E &= \frac{\text{total amount of Me in all extractants}}{\text{total amount of Me in initial source}} \times 100\% \\ &= \frac{m_{\text{Me,ex}}}{m_{\text{Me,0}}} \times 100\% \end{aligned}$$

In liquid–liquid extraction with the aqueous phase and organic phase, the percentage extraction % $E$  can be calculated by distribution ratio  $D$  as follows:<sup>34</sup>

$$\%E = 100D/(1 + D)$$



Jesús Esteban

*Jesús Esteban Serrano is Lecturer at the Department of Chemical Engineering of The University of Manchester. He earned his PhD in Chemical Engineering at the Complutense University of Madrid and was a postdoctoral researcher at the University of Birmingham, the Technical University of Dortmund and the Max Planck Institute for Chemical Energy Conversion. His newly founded research group approaches the sustain-*

*able production of value-added chemicals from renewable substrates focusing on Green Chemistry, Chemical Reaction Engineering and Process Intensification aspects. Additionally, he will develop research in separation processes using neoteric solvents. He has received multiple accolades, among which are the Green Talents Award of BMBF (2016), the Excellence Award in Chemical Reaction Engineering of the European Federation of Chemical Engineering (2018), the CAS Future Leaders Prize (2018), his mention in IUPAC's Periodic Table of Younger Chemists (2019) and the Hermann Neuhaus Prize of the Max Planck Society (2020).*





Fig. 1 Summary of the publication and citation reports for searches including the terms "eutectic solvent\*\*" and either "separation", "extraction" or "recovery" in the title or else "ionic liquid\*\*" and either "separation", "extraction" or "recovery" (a and b) as well as "metal recovery" or "metal extraction" or "metal separation" (c and d). Note that the terms are mutually exclusive to prevent duplicated references. Source: Web of Science.

## 2. Characteristics of DESs in relation with metal recovery

### 2.1. Classification of DESs

DESs were introduced as a family of solvents derived from ILs in the early 2000s by Abbott *et al.*, who described mixtures of components forming a eutectic, whose melting point is lower than those of the pure components.<sup>31,32</sup> This is depicted schematically in Fig. 2a, followed by the experimental data for  $\text{ChCl}:\text{EG}$  and  $\text{ChCl}:\text{Gly}$  as examples in Fig. 2b and c, respectively. Throughout the years, many more combinations of compounds have been found that follow such behavior and DESs have become a family of neoteric solvents by right.<sup>37</sup>

DESs feature large asymmetric ions with low lattice energy leading to the mentioned low melting points. They are obtained by the complexation of a compound that acts as hydrogen bond acceptor (HBA), typically a quaternary

ammonium salt, and either a metal salt or an organic compound that acts as hydrogen bond donor (HBD). Owing to the large combination of HBAs and HBDs possible, they can be tuned for the user's purpose and are thus considered designer solvents.<sup>39</sup> Fig. 3 depicts some common HBAs and HBDs.

DESs follow the notation  $\text{Cat}^+\text{X}^-\text{zY}$ , in which  $\text{Cat}^+$  stands for a cation (*e.g.*, ammonium, phosphonium, sulfonium) with  $\text{X}^-$  being a Lewis base serving as counter anion (mostly halide anions) and Y a Lewis or Brønsted acid of which  $z$  molecules interact with the  $\text{X}^-$  anion.<sup>39</sup>

With the following general formulas, DESs are classified into five types, namely:

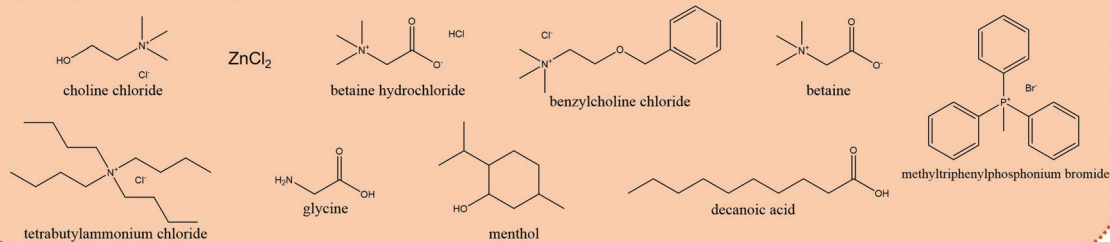
- Type I:  $\text{Cat}^+\text{X}^-\text{zMeCl}_x$ , where  $\text{Me} = \text{Zn}, \text{Sn}, \text{Fe}, \text{Al}, \text{Ga}$  or  $\text{In}$ . They are analogous to metal halide/imidazolium salt systems.
- Type II:  $\text{Cat}^+\text{X}^-\text{zMeCl}_x\cdot\text{yH}_2\text{O}$ , where  $\text{Me} = \text{Cr}, \text{Co}, \text{Cu}, \text{Ni}$  or  $\text{Fe}$ . The main difference with type I is that they form with hydrated metal halides, which also offer the possibility of decreasing the melting point in addition to being relatively inexpensive.





**Fig. 2** Representation of solid–liquid phase diagrams for DESs consisting of one HBD and one HBA. (a) General representation; (b) experimental melting points for ChCl: Eg and (c) experimental melting points for ChCl: Gly. The gray areas represent the concentration range for which the mixture is liquid at room temperature ( $T = 298.15$  K). Data for (b) and (c) were digitized and represented from ref. 38.

### Hydrogen bond acceptors



### Hydrogen bond donors

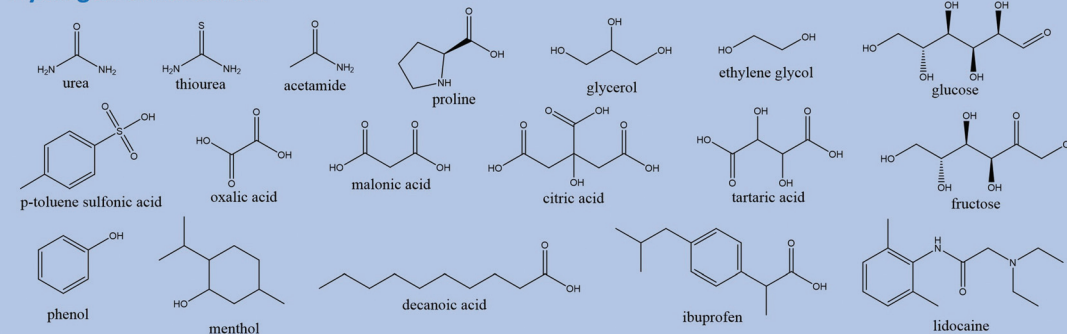


**Fig. 3** Some examples of common HBAs and HBDs present in the preparation of DESs.

• Type III:  $\text{Cat}^+\text{X}^-\text{zRZ}$ , where  $\text{Z} = \text{CONH}_2$ ,  $\text{COOH}$  or  $\text{OH}$  and  $\text{R}$  is an organic radical. They are by far the most widely known and applied. The vast majority generate with choline chloride (ChCl) and HBDs like amides, carboxylic acids and alcohols,

which make them easily tunable and normally inexpensive and in many cases biodegradable.

• Type IV:  $\text{MeCl}_x + \text{RZ} = \text{MeCl}_{x-1}^+\text{RZ} + \text{MeCl}_{x+1}$ , where  $\text{Me} = \text{Al}$  or  $\text{Zn}$  and  $\text{Z} = \text{CONH}_2$  or  $\text{OH}$ . These are mainly composed by



inorganic cations, which normally would not form low melting point eutectics. Examples of these include metal halides like  $\text{ZnCl}_2$  and HBDs like urea, acetamide or different diols.

• Type V. More recently, a new class was defined from the observation of the strong interaction from the acidity difference of phenolic and aliphatic hydroxyl moieties. Unlike in the previous types, the interactions between HBAs and HBDs are of non-ionic nature and, therefore, type V of this type of solvents are composed only of molecular substances. This is the case of the thymol-menthol system, to mention one example.<sup>40</sup>

To these more or less classic definition of DESs, different new terms have added more aspects more recently. Natural deep eutectic solvents (NADESS) would be one of them, which refers to type III DESs combining  $\text{ChCl}$  as HBA with naturally occurring carboxylic acids, sugars, aminoacids, adding water on some occasions as a third component.<sup>41–43</sup> Apart from  $\text{ChCl}$ -based NADESS, others can be prepared from binary or ternary mixtures of carbohydrates with themselves (e.g.  $\text{D-(-)-fructose} : \text{sucrose} (1 : 1)$  or  $\text{D-(+)-glucose} : \text{D-(-)-glucose} : \text{sucrose} (1 : 1 : 1)$ ) or organic acids with sugar alcohols (e.g., citric acid :  $\text{D-sorbitol} (1 : 1)$ ), among many others not requiring  $\text{ChCl}$ .<sup>44</sup> NADESS were conceived to study and possibly enhance the solubility of some intracellular compounds (flavonoid rutin, starch, albumin, *etc.*) that showed limited solubility in water.<sup>45</sup>

Additionally, therapeutic deep eutectic solvents (THEDESS) have emerged as another subcategory, where the particularity is that active pharmaceutical ingredients are one of the constituents and have potential interest in formulations, where solubility problems may be overcome.<sup>42</sup> In this way, for example, mixtures of menthol and ibuprofen have been proposed to enhance topical delivery systems.<sup>46</sup>

Concerning polarity, late investigations have included the use of hydrophobic<sup>47</sup> eutectic solvents, where the term “deep” can be dropped depending on the deviation from ideality of the eutectic point.<sup>48</sup> Hence, on occasions, they are referred to as hydrophobic (deep) eutectic solvents, H(D)ES. These arose when quaternary ammonium salts were combined with a long-chain carboxylic acid like decanoic acid, which conferred the resulting mixture hydrophobic properties. Further, H(D)ESs have included other carboxylic acids as well natural compounds like camphor, menthol, thymol as HBAs or HBDs.<sup>49,50</sup> In other cases, these H(D)ESs originate from the interaction of phenolic and aliphatic compounds, as explained for the type V of these neoteric solvents.<sup>40</sup>

## 2.2. Preparation and properties of DESs

The preparation of DESs is generally quite simple. They are synthesized by putting the HBD and HBA together and mixing at temperatures typically ranging between 50 and 100 °C for enough time to allow the hydrogen bonds to form and then allowing cooling down. It has been proposed to do the mixing of the components in two ways. One of them consists in allowing the component with the lowest melting point to melt and then add the other one with the highest melting point. When

both have similar high melting points, both are put together and mixed starting simultaneously.<sup>42</sup>

As already mentioned, DESs were initially considered a subclass of ILs. They have several similar properties, including the fact that their properties can be tuned for different applications. Commonly, they show very low vapor pressure, high viscosities, high chemical and electrochemical stability, and non-flammability. However, they are different in some crucial aspects that affect their implementation. ILs are generally more costly and complex to synthesize than DESs, which limits the use of the former in large-scale applications. On the other hand, the preparation of DESs has full atom economy and requires no purification. In addition, throughout the years, the biocompatibility, biodegradability and overall sustainability of ILs have been questioned, while DESs appear more promising in these regards.<sup>42</sup>

The design and optimization of the metal extraction process using DESs should be fundamentally based on the accurate and reliable information of their physicochemical properties (as shown in Fig. 4). Table 1 compiles available information on physicochemical properties of some selected DESs at 298.15 K, with particular focus on those that are known to have been used in metal separation and recovery applications. In these works, DESs based on  $\text{ChCl}$  have been used profusely, particularly those with HBDs like ethylene glycol ( $\text{ChCl} : \text{EG}$ , ethaline), glycerol ( $\text{ChCl} : \text{Gly}$ , glyceline) or urea ( $\text{ChCl} : \text{urea}$ , reline). Other references gather a good number of properties for some of these and other DESs,<sup>39,77–83</sup> including for the relatively recent H(D)ESs, for which solubility with water is crucial.<sup>49,84</sup> The table features values for the melting point ( $T_m$ ) of the DES together with viscosity, density, conductivity and surface tension, whose values can vary a lot depending not only on the specific HBAs and HBDs used, but also on the molar ratio.

**2.2.1 Density.** The density ( $\rho$ ) of DESs is a basic and important physical property to determine the solvent selection, process design, separation performance, as well as large-scale application of DESs for extractions in general considering the



Fig. 4 Important physicochemical properties of DESs for their application in metal recovery.



**Table 1** Physicochemical properties of selected DESs applied in the recovery of metals from different sources. Note: blank cells denote the lack of experimental data

HBA	m.p (°C)	HBD	m.p (K)	HBA : HBD	$T_m$ (K)	$\mu^a$ (51)	$\rho^a$ (g cm <sup>-3</sup> )	$\kappa^a$ (mS cm <sup>-1</sup> )	$\gamma^a$ (mN m <sup>-1</sup> )
ChCl	302	EG (ethaline)	260.20	2	207.15 (ref. 52)	37 (ref. 53)	1.12 (ref. 53)	7.61 (at 293.15 K) (ref. 54)	48.0 (ref. 53)
ChCl	302	Gly (glyceline)	290.95	2	233.15 (ref. 55)	259 (ref. 53)	1.18 (ref. 53)	1.32 <sup>b</sup> (ref. 55)	56.0 (ref. 53)
ChCl	302	Phenol		1 : 3	253.1 (ref. 56)	44.64 (ref. 56)	1.09 (ref. 56)	3.14 (ref. 56)	
ChCl	302	Fructose		2 : 1	283.15 (ref. 57)	11 800 <sup>a</sup> (ref. 57)	1.28 (ref. 58)		74.0 (ref. 58)
ChCl	302	Fructose		1 : 1	293.15 (ref. 57)	14 500 <sup>a</sup> (ref. 57)	1.34 (ref. 57)		70.5 (ref. 57)
ChCl	302	Glucose		2 : 1	288.15 (ref. 59)	9000 (ref. 59)	1.21 (ref. 59)		71.7 (ref. 59)
ChCl	302	Glucose		1 : 1	304.15 (ref. 59)	8000 (ref. 59)	1.27 (ref. 59)		73.1 (ref. 59)
ChCl	302	Maltose		1 : 1					
ChCl	302	Urea (reline)	407.15 (ref. 60)	1 : 2	285.15 (ref. 32)	750 (ref. 53)	1.25 (ref. 53)	2.31 (at 303.15 K) (ref. 61)	52.0 (ref. 53)
ChCl	302	Oxalic acid (oxaline)	463.15 (ref. 30)	1 : 1	307.15 (ref. 30)	1800 <sup>b</sup> (at 313.15 K) (ref. 30)		3.10 <sup>b</sup> (ref. 30)	
ChCl	302	Oxalic acid (oxaline)		1 : 2		458.4 (ref. 62)	1.24 (ref. 62)	1.88 (ref. 62)	
ChCl	302	Malonic acid (maline)	408.15 (ref. 30)	1	283.15 (ref. 30)	1124 (ref. 53), 828.7 (ref. 62)	1.25 (ref. 53)	0.91 (ref. 62)	65.7 (ref. 53)
ChCl	302	Citric acid	422.15 (ref. 30)	1	342.15 (ref. 30)	131 (ref. 63)	3.00 (ref. 63)	2.04 (ref. 64)	41.0 (ref. 63)
ChCl	302	Lactic acid		1 : 2	159.55 (ref. 63)	31 (at 303.15 K) [for 1 : 1] (ref. 66)	1.15 [for 1 : 1] (ref. 66)		
ChCl	302	Tartaric acid	444.15 (ref. 67)	2 : 1	195.42 (ref. 65)				
ChCl	302	Thiourea	443.15 (ref. 32)	1 : 2	320.15 (ref. 67)	2700 <sup>b</sup> (at 308.15 K) (ref. 68)	1.23 (ref. 69)		58.0 (ref. 69)
ChCl	302	PTSA		1 : 1	342.15 (ref. 32)	280 <sup>b</sup> (at 308.15 K) (ref. 70)	1.20 (at 308.15 K) (ref. 70)		
ChCl	302	PTSA		1 : 2		710 <sup>b</sup> (ref. 71)	1.25 (ref. 71)	0.60 <sup>b</sup> (ref. 71)	
[N4444]Cl or TBAC		Decanoic acid		1 : 3					
[N4444]Cl or TBAC		Decanoic acid		1 : 2		403 (ref. 72)		40.50 (ref. 72)	
Betaine		Glycerol (Gly)		1 : 3	380.00 <sup>b</sup> (ref. 73)	2600 <sup>b</sup> (ref. 64)	1.22 (ref. 64)	1.00 <sup>b</sup> (ref. 64)	
Citric acid		Glucose		1 : 1			1.45 (ref. 74)	4.90 <sup>c</sup> (ref. 74)	
Citric acid		Sucrose		1 : 2	227.20 (ref. 75)	7000 <sup>b</sup> (ref. 75)	1.43 (ref. 75)	62.60 <sup>c</sup> (ref. 74)	
ZnCl <sub>2</sub>		Acetamide	361.15 (ref. 76)	1 : 4	257.15 (ref. 76)	350 <sup>b</sup> (ref. 76)	1.36 (ref. 76)	320.00 <sup>b</sup> (ref. 76)	53.0 <sup>b</sup> (ref. 76)
ZnCl <sub>2</sub>		EG		1 : 4		150 <sup>b</sup> (ref. 76)	1.45 (ref. 76)	345.00 <sup>b</sup> (ref. 76)	57.0 <sup>b</sup> (ref. 76)
ZnCl <sub>2</sub>		Urea	407.15 (ref. 76)	1 : 3.5	282.15 (ref. 76)	22 000 <sup>b</sup> (ref. 76)	1.63 (ref. 76)	50.00 <sup>b</sup> (ref. 76)	72.0 <sup>b</sup> (ref. 76)

<sup>a</sup> At  $T = 298.15$  K unless otherwise noted. <sup>b</sup> Values from digitizing images. <sup>c</sup> From fitting equation.

biphasic nature of this unit operation. For large-scale applications, the density of the DESs is an essential parameter for the procedure design, size of devices and containers calculation, overflow evaluation, and cost estimation.<sup>85</sup> In general, the densities of DESs are greater than that of water and, as such, the DES-rich phase is normally the heavy liquid at the bottom, although that is not always the case. For instance, the

extract-rich H(D)ESs phases are usually collected from the upper liquid phase in liquid–liquid metal extraction from aqueous solutions since the H(D)ESs usually have a lower density than water (in the range 0.90 to 0.95 g cm<sup>-3</sup>).<sup>86</sup>

The fine control of the DES density can be achieved through varying the types of individual component and their molar ratios.<sup>85,87</sup> DESs based on bromine salts generally have





higher densities than their chlorine salt counterparts, indicating that the anionic type would affect the DESs densities.<sup>85</sup> Besides, the densities of DESs composed of hydroxyl HBDs exhibited an increasing trend with the number of hydroxyl groups (*e.g.*, the glycerol (Gly)-based DESs are denser than EG-based ones). In contrast, the reduction of the DESs densities can be achieved by introducing the aromatic groups (*e.g.*, phenolic-based DESs have low densities) and increasing the alkyl chain length of the DESs components (*e.g.*, the densities of diacid-based DESs follow the order of oxalic acid (C<sub>2</sub>H<sub>2</sub>O<sub>4</sub>)-based > malonic acid (C<sub>3</sub>H<sub>4</sub>O<sub>4</sub>)-based > glutaric acid (C<sub>5</sub>H<sub>8</sub>O<sub>4</sub>)-based).<sup>78</sup> As for the molar ratios of the components, it has been extensively reported that the density of DES would significantly increase with the increasing ratios of the HBDs.<sup>63,88,89</sup> For example, Shafie *et al.* (2019) observed that the densities of ChCl: citric acid monohydrate DESs increased dramatically from 2.64 to 3.11 g cm<sup>-3</sup> when the molar ratios of HBA: HBD changed from 2:1 to 1:3.<sup>63</sup> This could be explained by the theory that the higher ratios of HBD would provide the stronger hydrogen bond interaction between HBA and HBD, resulting in the reduction in the free space, or called the average “hole” radius, and the change of the packing efficiency/molecular arrangement of DESs.<sup>54,63,89</sup> Additionally, the DESs densities also vary with the temperature since the change of molecular activity and mobility with the temperatures will impact the DESs volumes and thus their densities. In general, the densities and molar volumes of DESs decrease and increase linearly, respectively, with increasing temperature.<sup>89,90</sup>

**2.2.2 Viscosity.** Viscosity ( $\mu$ ) is another critical property of DESs as it affects mass transfer in separation applications with DESs.<sup>91</sup> As in the case of ILs, the higher  $\mu$  of DESs, as compared to most conventional molecular solvents such as water, is originated from the large size of the ions and the relatively high free volume.<sup>39</sup> Low viscosities indicate weak molecular interactions of the DESs components which may decrease the freezing point and the solubility.<sup>85</sup> Accordingly, the tuning of DESs viscosity should take into account the balance between transmission performance and solvation properties, which requires a deeper understanding of DESs. Previous studies have extensively reported that the viscosity of DESs can be customized by varying their composition since the structures and molecular ratios of HBAs and HBDs in DESs have determining effects on DESs viscosities. For instance, within the ammonium-based DES with Gly as HBD, the viscosities of the DESs increased with their molecular weights.<sup>92</sup> The viscosities of the ammonium-ChCl-based DESs would significantly decrease with higher molar ratios of EG, but increase with the malonic acid (MA) content when using the mixture of EG and MA as HBDs. This could be explained by the variation in the strength of hydrogen bond interaction between HBA and HBD.<sup>89</sup> In addition, it has been reported that most DESs retain their typical network of hydrogen bonds with a water content up to *ca.* 42 wt%.<sup>93,94</sup> Thus, the viscosity of a DES could be reduced with the addition of a small amount of water.<sup>95</sup>

In addition to the composition of the DES,  $\mu$  is also temperature-dependent, and as in the case of molecular solvents,

the dependence is generally expressed by models described with Arrhenius, Vogel–Tamman–Fulcher or Andrade equations.<sup>89</sup>  $\mu$  generally decreased with temperature, which could be attributed to the decrease in internal resistance of molecules causing the molecules easy to flow.<sup>60</sup>

Many studies have reported how crucial this variable is on metal separations. Doche *et al.* (2017) studied the effects of temperature on the leaching rate of Co in ethaline.<sup>96</sup> The leaching rate at 80 °C was 15 times higher than that at 25 °C, which resulted from the decrease in  $\mu$  of ethaline. Zhu *et al.* (2019)<sup>5</sup> also reported that the dissolution efficiency of Zn in a ChCl-based DES increased from 48.5% to 85.2% with temperature increases from 60 to 80 °C. The leaching process was controlled by diffusion through a liquid phase boundary layer with relatively high activation energy, which was caused by high  $\mu$  of the ChCl-urea-EG solvent.<sup>97</sup> Additionally, the dissolution of Co in ethaline was found to be highly dependent on the temperature, as the Co leaching efficiency was negligible with extraction temperatures lower than 120 °C and increased to 99.3% with temperature increased to 180 °C. The leaching of LiCO<sub>2</sub> in ethaline involves the simultaneous oxidation of EG and reduction of Co, generating different compounds under different temperatures.<sup>98</sup> Roldán-Ruiz *et al.* (2020) also reported that the dissolution efficiency of LiCO<sub>2</sub> in PTSA-based DES increased from approximately 40% to 95% with temperature increased from 50 to 120 °C.<sup>97</sup> Overall, the  $\mu$  of DESs can be reduced with the increase of temperature; however, decomposition of DES may be observed at high temperature. For instance, Zürner and Frisch (2019)<sup>161</sup> explored the effect of temperature on leaching In, Sn and Zn flue dust by oxaline. The flowability of DES was severely impeded due to high  $\mu$  at temperature below 50 °C, while slow decomposition of oxaline was observed at temperature above 80 °C.

**2.2.3 Conductivity.** Since electrodeposition is an important process for the recovery of metal dissolved in DESs, the conductivity ( $\kappa$ ) of DESs is an essential property to evaluate their eligibility to serve as successful electrolytes.  $\kappa$  is closely related to the state of free ions as well as the ion migration rates in the solvents.<sup>85</sup> This property varies with temperature,  $\mu$  and the size of ions, which can be attributed to the “hole”, or free space, theory.<sup>99,100</sup> Ghareh Bagh *et al.* (2015)<sup>101</sup> measured the conductivity profiles of sixteen DESs, and observed a consistent trend of increasing with temperature, which could be attributed to the higher kinetic energy and migration rate of the molecules at the elevated temperature.<sup>89</sup> Further,  $\kappa$  increased significantly as viscosity decreased due to the free mobility of ionic species as the hole mobility increased; thus, ammonium-based DESs with lower viscosities tended to have higher  $\kappa$  than phosphonium-based DESs.<sup>92</sup> In addition, decreasing the size of the ions could increase the free volume of DESs, and thus reduce the viscosity and improve the conductivity.<sup>99,102</sup> For example, the smaller-size ammonium-based DESs had higher electrical conductivities than the phosphonium-based DES, making them more suitable as solvents and electrolytes in electrolysis processes.<sup>101</sup> The relationship among conductivity, viscosity and temperature can be described by the Walden rule.<sup>85</sup>



**2.2.4. Thermal and chemical stability.** The stability of the solvents directly affects their reusability and performance in large-scale applications.<sup>103</sup> DESs have been reported to have relatively good thermal and chemical stability, which rely on the molar ratios, spatial structure, and functional groups of their compositions.<sup>85</sup>

The thermal stability of DESs can be evaluated by the decomposition temperature, which is usually measured by the thermogravimetric analysis (TGA). Besides, the two major analytical methods for further evaluation of thermal stability of DESs include: (1) the evaluation of alteration of the physico-chemical characteristics as a function of temperature increment, and (2) measurement of the mass loss as a function of time at a constant temperature.<sup>90,104–106</sup> The decomposition temperature represents the upper-temperature limit of a DES existing as a fluid without any deterioration of its physico-chemical properties.<sup>89,90</sup> Thus, a higher decomposition temperature is desirable for DESs as it indicates that they can be used at a higher temperature with better thermal stability. The decomposition temperatures of some common-used DESs, such as choline acetate:Gly (1:1.5), ChCl:urea (1:2) and ChCl:Gly (1:2), are in the range of 205–216 °C.<sup>107</sup> ChCl:EG and ChCl:DMF exhibited much higher decomposition temperature (>300 °C) than ChCl:DMSO (<100 °C) and ChCl:lactic acid (<127 °C).<sup>108</sup> It has been reported by several studies that the thermal stability of the DESs was strongly affected by intermolecular hydrogen bondings formed between HBAs and HBDs as well as the intrinsic thermal stability of the compositions.<sup>85,109</sup> For example, the thermal stability of the ChCl-based DESs with organic acids as HBDs depends on the number of hydrogen bonds provided by the acids and the thermal stability of the organic acid itself.<sup>85</sup> Accordingly, the thermal stability of several ChCl-based DESs followed the order of ChCl:tartaric acid > ChCl:lactic acid > ChCl:malonic acid.<sup>110</sup> Pateli *et al.* (2020) found that the thermal stability of the DESs composed of ChCl, malonic acid and EG improved with the increase in the molar ratio of malonic acid due to the enhanced formation of hydrogen bonds.<sup>109</sup> However, it should be noted that the all-encompassing rules could not be drawn for all the DESs and they should be carefully studied on a case-by-case basis. Taking the trioctylphosphine oxide (TOPO)-based DESs as example, the TOPO:malonic acid DESs showed poorer thermal stability than the neat acid because of a self-catalyzing effect, while the TOPO:levulinic acid DESs were obviously more thermally stable than the neat levulinic acid as the mixtures prevented the decomposition by dehydration.<sup>90</sup>

The chemical stability of DESs refers to the potential changes in compositions or properties due to chemical reactions (*e.g.*, oxidation, hydrolysis, *etc.*). The hygroscopic property is one of the main concerns for the chemical stability of DESs, especially for the hydrophilic DESs like ChCl-based DESs.<sup>111</sup> Schaeffer *et al.* (2020) evaluated the chemical stability of the non-ionic hydrophobic DES (*i.e.*, TOPO:thymol) and its impact on the extraction of several metals (*i.e.*, Pt, Pd and Fe) by <sup>1</sup>H-NMR and <sup>13</sup>P-NMR respectively, which confirmed the

stability of the TOPO:thymol mixture under acidic conditions and suggested that metal extraction occurred only when an excess of TOPO was present.<sup>86</sup> The chemical stability of DESs is the prerequisite for thermal stability and is of great importance for industrial applications. Especially for the transportation and long-time storage or operation during large-scale applications, excellent chemical stability of DESs is desirable to reduce the safety risks and improve the cost-effectiveness of the DESs-based metal extraction process.<sup>85</sup>

**2.2.5. Hydrophilicity/hydrophobicity.** DESs can be categorized into hydrophilic and hydrophobic DESs based on their affinity to water, which is determined by the nature and interactions of the HBAs and HBDs.<sup>85,104</sup> In general, early developed DESs synthesized by ChCl as HBA and alcohols, carboxylic acid or amides (*e.g.*, urea) as HBD show hydrophilic characteristics due to the abundance of hydrogen bondings and coulombic interactions, leading to their completely miscible with water.<sup>85,90</sup> On the contrary, hydrophobic eutectics (H(D)ESs) are often composed of naturally sourced and intrinsically hydrophobic terpenes (such as menthol and thymol), trialkylphosphine oxide, or tetra alkyl-quaternary-ammonium salt as HBAs and various HBDs including long-chain carboxylic acid (*e.g.*, decanoic acid), which have low water solubility.<sup>85,104,112,113</sup>

In most previous studies, the hydrophobicity/hydrophilicity screening test were carried out on different DESs combinations to screen out the appropriate ones with suitable hydrophilicity/hydrophobicity before the evaluation of their potential applications. For example, Geng *et al.* (2019)<sup>114</sup> mixed 5 hydrophilic low alkyl chain quaternary ammonium ILs (*i.e.*, [N<sub>1111</sub>]Br, [N<sub>2222</sub>]Br, [N<sub>3333</sub>]Br, [N<sub>4444</sub>]Br, and [N<sub>8881</sub>]Br) with a series of HBDs (*i.e.*, decanoic acid, 1-propyl alcohol, EG, Gly, 1-hexanol, and *N*-hexanoic acid) in a molar ratio of 1:1 to construct H(D)ESs. To evaluate the hydrophobicity of the combined products, they were mixed with deionized water for 30 min followed by centrifugation for 20 min. As a result, H(D)ESs formed two stable phases without volume loss. The results listed in Table 2 showed that the more potential hydrophobic combinations of DESs could be obtained with the longer alkyl chain of HBAs (*i.e.*, [N<sub>4444</sub>]Br, and [N<sub>8881</sub>]Br), while the hydrophobicity of DESs can be further improved by increasing the hydrophobicity of the HBD reagents. Tang *et al.* (2021)<sup>115</sup> also screened suitable H(D)ESs by a similar hydrophobicity screening test on the [N<sub>8881</sub>]Cl-based DESs with different types of saturated fatty acids and alcohols as HBDs. The water contents corresponding to the DESs before and after mixing with water were also determined by titration to quantitatively evaluate the hydrophobicity of the DES candidates, which showed that DES N<sub>8881</sub>Cl:1-octanol (1:2) has the least water content and the highest hydrophobicity, resulting from the longest saturated fatty chain of 1-octanol among all the HBDs of the studied DESs.

The hydrophilicity/hydrophobicity of DESs is a critical factor affecting their applications in metal extraction and separation. Conventional DESs synthesized by ChCl, Gly, urea, or EG, are all hydrophilic solvents. Hydrophilic DESs are more



**Table 2** Status of composed DESs after hydrophobicity tests. The squares with "solid" marked: solid (under room temperature); the squares with "X": hydrophilic; the square with "/": cloudy status shows; the unmarked squares: hydrophobic. Reprint with permission from ref. 114, Copyright © 2019, Elsevier B.V

	Decanoic acid	1-Propyl alcohol	Ethylene glycol	Glycerol	1-Hexanol	N-Hexanoic acid
[N <sub>1111</sub> ]Br	Solid	X	/	/	X	X
[N <sub>2222</sub> ]Br	Solid	X	/	/	X	X
[N <sub>3333</sub> ]Br	Solid	X	/	/	X	—
[N <sub>4444</sub> ]Br	Solid	X	/	/	—	—
[N <sub>8881</sub> ]Br	Solid	X	—	—	—	—

suitable in solid and nonaqueous liquid samples for metal dissolution.<sup>85,115</sup> The ChCl-based hydrophilic DESs with urea, carboxylic acid (e.g., malonic acid or citric acid), and EG as HBDs have exhibited great performance for dissolution and leaching of various commonly available metal oxides,<sup>89,116</sup> precious metals (e.g., Au)<sup>117</sup> and valuable rare earth elements (e.g., Y, La, Ce, Nd and Sm)<sup>91</sup> from ores or metal-bearing solids. Additionally, the hydrophilic DESs have also been applied as electrolytes for electrochemical dissolution of metals (e.g., Sn, Pb, Zn, Cu, Co, etc.), such as anodic dissolution<sup>109,118</sup> and electrodeposition.<sup>119–122</sup> The advantages of hydrophilic DESs as electrolytes for the electrochemical process include nonacidic formulation, the improved surface finish on cast pieces, and enhanced current efficiency.<sup>123</sup>

In contrast, metal extraction and recovery from water-soluble environments require H(D)ESs, since they are immiscible with water and have high extraction efficiency for non-polar analytes.<sup>41,80,85,124</sup> Since a (H)DES synthesized by decanoic acid and lidocaine was first reported by van Osch *et al.* in 2015,<sup>125</sup> this type of solvents have been extensively employed as promising extractants for metals from a variety of aqueous samples.<sup>104,115,126</sup> For example, H(D)ESs were prepared by decanoic acid and lidocaine to remove  $\text{Co}_2^+$  in water with an extraction efficiency higher than 99%.<sup>127</sup> Schaeffer *et al.* (2018) reported that the H(D)ES consisting of terpenes and fatty acids showed highly selective towards  $\text{Cu}^{2+}$  when it was used as an extractant in concentrated solutions containing other transition metals.<sup>113</sup> Geng *et al.* (2019) employed hydrophobic DESs based on quaternary ammonium salts for Au recovery and achieved 96.8% extraction efficiency of Au from 1 mM Au(III) solution.<sup>114</sup> Overall, these H(D)ESs could effectively extract metals with high efficiency, and it was also reported that the metal recovery by H(D)ESs could reach equilibrium rapidly within five seconds.<sup>87</sup> Moreover, the water content increased from 0.15 wt% in the original solvents to only 2.50 wt% after extraction.<sup>113</sup> Thus, the H(D)ESs showed high recyclability during the extraction cycles due to the negligible solubility of their hydrophobic components in water. Furthermore, with the recent introduction of non-ionic H(D)ESs, these appear as an interesting alternative in terms of sustainability owing to their favourable toxicity profile compared to some ILs and conventional organic solvents.<sup>85,86,128</sup> Examples of these would be mixtures of two different bio-sourced terpenes,<sup>48</sup> the mixtures of thymol or menthol with carboxylic acids,<sup>113</sup> and the mixtures of trioctylphosphine oxide (TOPO) with phenol.<sup>86</sup>

**2.2.6. Acidity.** Another critical parameter influencing the metal extraction performance of DESs is their acidity. The acidity of DESs can be determined by employing UV-Vis spectroscopy to measure the ratio of absorbances for the protonated and deprotonated forms of indicator.<sup>129</sup> To quantify acidity, the Hammett function has been used, as in the case of other organic solvents. The acidity of DESs could be provided by the organic acids HBDs (e.g., carboxylic acid, sulfonic acid).<sup>85</sup> It was shown that the more acidic DESs solubilized metal oxides better. For example, the DESs synthesized with organic acids (*i.e.*, glycolic acid and L-lactic acid) could more efficiently dissolve  $\text{Nd}_2\text{O}_3$  compared to others prepared by Gly and EG.<sup>130</sup>  $\text{Fe}_3\text{O}_4$  showed a higher tendency to be dissolved in stronger acidic DESs composed of ChCl : oxalic acid rather than in ChCl : phenylpropionic acid, and aluminates had higher solubility in malonic acid-based DESs than in urea and EG-based DESs.<sup>83,85</sup> Pateli *et al.* (2020) used a superacid ( $\text{p}K_a \approx 15$ ), trifluoromethanesulfonic acid (TFSA), to change the acidity of ethaline for systematically investigating the role of proton activity of DESs in the dissolution of metal oxides, such as MnO, CoO, NiO, CuO,  $\text{Cu}_2\text{O}$ , ZnO, PbO, *etc.*<sup>129</sup> All the selected metal oxides in this study exhibited a strong acidity dependency on dissolution, *i.e.*, the higher dissolution of metal oxides was obtained in higher acidity (lower pH) of the DESs, and the activity of  $\text{H}^+$  was identified as a major limiting factor for metal oxide dissolution in DES media with poorly coordinating HBDs. This was because the protons in DESs acted as oxygen acceptors and higher concentrations of  $\text{H}^+$  were required to react with the  $\text{O}^{2-}$  and break the metal-oxide bonds.<sup>129</sup>

### 3. Review articles dedicated to the applications of DESs in various fields

In relation with the properties described above, DESs have attracted a great deal of attention in many applications. Remarkably, they have also gained industrial relevance as the number of patents granted using these chemical compounds has increased in the last few years.<sup>41</sup> In particular, type III DESs with ChCl as HBA have been widely studied given their inexpensiveness and easy biodegradability. In academic research, the increasing efforts on the use of DESs have led to the release of a good number of reviews. Table 3 summarizes the most relevant reviews that have appeared in the past few



**Table 3** Summary of reviews found in the open literature on the use of DESs for different applications and the main aspects covered

Type	Focus of the review on DESs	Main points covered	Ref.
Chemical reaction	DESs as reaction media and catalysts	<ul style="list-style-type: none"> <li>Physicochemical properties of some typical DESs</li> <li>Mechanisms and insights into the role of DESs as catalyst or reaction media in additions, cyclizations, replacements, condensations, oxidations and reductions among other.</li> </ul>	79, 131 and 147
Separation processes	Separation of aromatic and aliphatic hydrocarbons	<ul style="list-style-type: none"> <li>Comparison of the performance of DESs with ILs and other organic solvents.</li> <li>Use of COSMO-RS as solvent screening tool for DESs</li> </ul>	133
Separation processes	Desulfurization of liquid fuels	<ul style="list-style-type: none"> <li>Physicochemical properties of some typical DESs</li> <li>Mechanisms of desulfurization using DESs</li> <li>Variables affecting efficiency of extraction: HBA and HBD, temperature, time, regenerability of DESs</li> </ul>	137
Separation processes	Separation of bioactive compounds	<ul style="list-style-type: none"> <li>Physicochemical properties of selected DESs and NADESs</li> <li>Extraction of different polyphenols, polysaccharides, proteins, terpenoids, <i>etc.</i></li> <li>Use of process intensification in combination with DESs: microwaves, ultrasounds, ball mill, <i>etc.</i></li> </ul>	80 and 138
Separation processes	Extraction techniques with hydrophobic (D)ES	<ul style="list-style-type: none"> <li>Properties of hydrophobic (D)ESs</li> <li>Liquid phase, ultrasound and microwave-assisted microextraction</li> <li>Liquid-liquid and solid-phase extraction</li> <li>Different types of dispersive and single drop microextractions</li> </ul>	84
Separation processes	Gas separation with attention to CO <sub>2</sub> <sup>139</sup> and SO <sub>2</sub> <sup>78</sup>	<ul style="list-style-type: none"> <li>Physicochemical properties of some typical DESs</li> <li>Comparison of absorption of CO<sub>2</sub> and SO<sub>2</sub> in DESs and ILs</li> <li>Thermodynamic analysis of the absorption process</li> <li>DESs as catalysts in the transesterification reaction</li> </ul>	78 and 139
Biotechnology and biorefinery	Biodiesel production	<ul style="list-style-type: none"> <li>DESs as extracting solvents of glycerol for biodiesel purification</li> <li>Role of the different type of DESs on biomass fractionation, going in detail to the type of HBA and HBDs. Also, ternary DESs.</li> <li>Integration of the use of DESs in biomass fractionation with microwave, ultrasound, hydrothermal and biological pretreatments</li> <li>Pretreatment of solid fraction</li> <li>Upgrading of lignin fraction with DESs</li> </ul>	140 and 141
Biotechnology and biorefinery	Lignocellulosic biomass fractionation	<ul style="list-style-type: none"> <li>Mechanisms of lignin and cellulose depolymerization</li> <li>Effect of specific DESs on lignin extraction and saccharification enhancement.</li> </ul>	142
Biotechnology and biorefinery	Lignocellulosic biomass pretreatment: lignin extraction and saccharification	<ul style="list-style-type: none"> <li>Toxicity and biodegradability of DESs</li> </ul>	143
Biotechnology and biorefinery	Biotechnology, bioengineering and biocatalysis	<ul style="list-style-type: none"> <li>Separation of natural products with DESs</li> <li>Biocatalysis using DESs as solvents</li> <li>DESs as catalysts</li> <li>Preservation of biological materials in DESs</li> <li>Pharmaceutical, therapeutical and biomedical applications of DESs</li> <li>Role in metal processing and deposition</li> <li>Role as reaction media for the synthesis of nanoparticles</li> </ul>	41, 144 and 145
Advanced materials	Applications in nanotechnology	<ul style="list-style-type: none"> <li>Definitions of different types of DESs</li> </ul>	77
Advanced materials	Production and application of polymers, metals and nanomaterials	<ul style="list-style-type: none"> <li>Role as solvents, functional additives and monomers in the production of polymers</li> <li>Physicochemical properties of many DESs and H(D)ESs</li> </ul>	42
Separation processes, reaction and materials	Very comprehensive review covering environmental, health and food related detections, separation of bioactive compounds and applications in material preparations.		146



Table 3 (Contd.)

Type	Focus of the review on DESs	Main points covered	Ref.
Novel types of DESs	Natural deep eutectic solvents (NADESS)	<ul style="list-style-type: none"> <li>• Application in detection technology for food safety and environmental protection.</li> <li>• Separations in metallurgy, chemical and fermentative processes.</li> <li>• Effect of DESs in advanced materials and energy storage and conversion.</li> <li>• Properties and comparison of NADESSs with ILs and DESs</li> <li>• Interaction of NADESSs components</li> <li>• Preparation of NADESS</li> <li>• Applications as extraction and chromatographic media and in biomedicine</li> </ul>	43
Novel types of DESs	Hydrophobic <sup>47</sup> (deep) eutectic solvents	<ul style="list-style-type: none"> <li>• Formulation, preparation and types of H(D)ESs</li> <li>• Physicochemical properties</li> <li>• Some applications in the extraction of natural compounds</li> </ul>	49

years classified by type of application highlighting the main features covered in each of them.

DESs have been widely applied as essential elements in a good number of chemical reactions. Their use as solvents has improved the performance of different reactions in terms of selectivity or stereoselectivity to the desired products or sometimes moderating the reaction conditions. The role of DESs in the mechanism is discussed for different addition, cyclizations, replacement, condensation, reduction and oxidation reactions.<sup>79,131</sup> One particular example of interest for metal recovery would be the use of the ChCl:Gly (glyceline) and ChCl:urea (reline) DESs, which have shown a good capacity of retaining rhodium complexes in the biphasic hydroformylation of olefins with the purpose of homogeneous catalyst recycling.<sup>132</sup>

DESs have proven outstanding sustainable media to undertake different separations with a great degree of selectivity. For instance, DESs have proven effective, on occasions even more than ILs, in the separation of aromatics and aliphatics in hydrocarbon mixtures. This purification processes represent a challenge given the differences of the boiling points and the existence of azeotropes, which makes distillation a costly operation. A review by Hadj-Kali *et al.* (2017) presents a large comparison of DESs with ILs and organic molecular solvents in extraction processes to separate the mentioned classes of compounds.<sup>133</sup> What is also of relevance is that they cover the use of the conductor-like screening model for real solvents (COSMO-RS) theory<sup>134,135</sup> as a tool to analyze and predict the separation performance of DESs and molecular solvents. This approach has been used in numerous other works, accentuating the use of this tool to comply with the principles of Green Chemistry.<sup>24,136</sup> However, it must be noted that the COSMO-RS theory is not capable of predicting equilibria in systems containing metals. Further in mixtures related to hydrocarbons, DESs have been used profusely in the desulfurization of fuels, a problem of great concern for atmospheric emissions.<sup>137</sup> In extraction processes, DESs and NADESSs have also been employed to separate different bioactive compounds from organic matrices like polyphenols, proteins, terpenoids or

asthaxanthin, also analyzing the effect of adding different amounts of water to DES or the use of process intensification, both of which can help enhance extraction efficiency.<sup>80,138</sup> Further, a recent review has covered the application of H(D)ESs in microextraction techniques, summarizing their application in environmental samples (water from different origins), food samples or human samples (plasma, urine) among other examples. The operation procedures as well as analytical techniques used are given in great detail.<sup>84</sup>

DESs have also been widely applied in the absorption of gases, such as CO<sub>2</sub><sup>78,139</sup> or SO<sub>2</sub>.<sup>78</sup> The performance of DESs as media for gas sweetening has been summarized and compared to other molecular solvents and ILs; in addition, thorough thermodynamic insights into the equilibria and the influence of HBAs and HBDs are given.

In a quest for a more sustainable production of chemicals, DESs have been put to use in the context of biotechnologies and biorefineries. The use of these solvents has been implemented in the production of biodiesel mainly with two purposes. First, they can act as catalysts to initiate the corresponding transesterification reaction. The second use is to make a DES, mainly using ChCl to separate Gly, the by-product of the production process.<sup>140,141</sup> The roles of DESs has also been reported in the fractionation of lignocellulosic biomass as agents pretreat the solid raw materials and obtain separately the cellulosic, hemicellulosic and lignin components, which can then undergo different transformations to value-added products.<sup>142,143</sup> Last, the toxicity and biodegradability of DESs have been assessed thoroughly, leading to their characteristics being favorable for application as solvents in biocatalysis, the preservation of biological materials and the composition of pharmaceuticals. DESs have been found to reproduce the environment in cells, mimicking metabolites and forming a different type of liquid besides water and lipids. In addition, it appears that protein structure could be better preserved in DES than other organic solvents.<sup>41,144,145</sup>

In the field of nanotechnology, DESs have been used in two major ways. First, as media to disperse nanoparticles and control morphology, and second as reaction media for nano-



material production. Application of DESs as precursor solvents in nanoparticle synthesis can enhance the stability and yield materials with uniform surface, small size, and highly mesoporous as well as highly crystalline nature.<sup>77</sup> Similarly, they have been used for the production of advanced materials like polymers and in metal processing.<sup>42</sup>

It is worthwhile mentioning a recent comprehensive review by Cao and Su, which compile several of the aspects mentioned above. Their work covers the use of DESs for a wide variety of fields, such as separations in food and environmental samples, separations in chemical and biocatalytic processes or the preparation of advanced materials, including for energy storage and conversion.<sup>146</sup>

Last, two reviews have focused specifically on the definition of NADESS<sup>43</sup> and H(D)ESS<sup>49</sup> putting the spotlight on their preparation and characteristics together with their main differences with the other types of DESs.

As summarized in this section, DESs have shown very promising results in several applications. Their relevance in metal recovery research from different sources remains to be reviewed, so the next section will describe their use in this type of endeavors.

## 4. DESs in metal recovery and separation

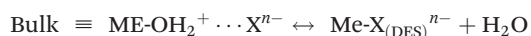
### 4.1. Mechanisms of DESs for metal recovery

The mechanisms behind the separation of metals by DESs have been investigated recently. In general, the dissolution of metal oxide in DESs can be regarded as a two-step process:<sup>35,129,148</sup> (1) the protons of the functional groups in HBDs (*e.g.*, the carboxyl groups of organic acid and the hydroxyl group of alcohol) of DESs first react with the active OH sites of the hydrated metal oxide to form intermediate species with protonated oxide, which can be expressed as follows:



where “Bulk  $\equiv$  Me-OH” stands for the hydrated metal oxide with active OH sites; HX is the HBDs of DESs.

(2) If the metal–ligand complexes are more stable than the metal–OH complex, the protons would break the metal–oxide bonds. The deprotonated HBDs ligand would substitute the OH active sites for metal–ligand complexation, followed by ligand exchange for anion (*e.g.*, Cl<sup>−</sup>) in the bulk DESs:



Abbott *et al.* (2006) compared the solubilities of 17 transition metal oxides of period 4 in three ChCl-based DESs (*i.e.*, ChCl: malonic acid (maline), reline and ethaline) with those found in aqueous solutions (*i.e.*, 0.181 M NaCl and 3.14 M HCl aqueous solution).<sup>116</sup> For most metal oxides, the solubilities are in the order HCl > maline > reline > NaCl > ethaline, which is nearly in line with the order of proton activity in these

extractants. The Analogous manners could be observed in both DESs and aqueous solvents where the more ionic oxides, such as ZnO, had higher solubilities than the more covalent oxides, such as TiO<sub>2</sub>. Good correlation between the solubilities of metal oxides in DESs and their intrinsic properties (including heats of fusion, melting points, the charge on the metal, and the crystal ionic radius)<sup>116</sup> as well as their stability<sup>129</sup> was also observed. Metal oxides with lower stability would have smaller lattice energies between the oxygen anion and the metal cation and less negative Gibbs energy of formation, and thus, would be more prone to be attacked by the protons from DESs.<sup>129</sup> Moreover, the solubilities of the oxides in the DESs, especially maline, correlated well with those in aqueous HCl, but did not correlate with aqueous NaCl solution.<sup>116</sup> These behaviors indicated that the dissolution of metal oxide should be more related to the presence of protons in DESa, as explained by the aforementioned step of dissolved of metal oxide in DESs as the oxygen acceptor and thus changed the complex formed. Besides, the second step of metal oxides dissolution in DESs involving the formation of metal–ligand complexes that the dominant forms of metals detected in DESs were chlorometalate species in the form of [MeCl<sub>x</sub>]<sup>(n−)</sup>.<sup>35,116</sup> Furthermore, the formation of the anionic metal chloro complexes is also accounted for the dissolution of some poorly soluble metal salts in the DESs. For example, AgCl dissolved in ethaline in the form of [AgCl<sub>2</sub>]<sup>−</sup> complex with a solubility around 0.2 mol kg<sup>−1</sup>, causing a potential shift of the Ag/AgCl reference electrode in DES as reported by Shen *et al.* (2020).<sup>149</sup>

Accordingly, it could be concluded that the dissolution of metals in DESs should be largely determined by the proton activity and complexation abilities of the DESs, which could be modulated by adjusting the HBDs and HBAs and their molar ratio in DESs. Some research efforts have been devoted to investigating the metal dissolution in various DESs with different HBDs.<sup>53,116,129,148,150,151</sup> It has been reported that ChCl-based DESs are capable of dissolving various metal oxides, with the solubility being largely dependent on the nature of the HBDs. The modification of HBDs can induce changes in the solubility of up to several orders of magnitude. For example, the maline exhibited the higher ability compared to reline and ethaline in the dissolution of most of the commonly available metal oxides shown in Fig. 5a.<sup>116</sup> This result could be further explained from two aspects: (1) the high polarity with highly active dissociated protons of malonic acid in maline could act as good oxygen acceptors, leading to strong H-bonding interactions and formation of chlorometalate species.<sup>35,116</sup> (2) The occurrence of dimerization phenomena, which refers to the formation of extensive chains of dimers rather than single dimer units due to the two carboxylic acid functional groups in the malonic acid molecules, would result in the similar mobility of the HBD (*i.e.*, malonic acid) with the choline cation, and lead to the strong complexation ability.<sup>53</sup> Hartley *et al.* (2014) further investigated the speciation of 25 metal salts in 4 ChCl-based DESs (with 1,2-ethanediol, 1,2-propanediol, 1,3-propanediol and urea as HBD) using extended X-ray absorption fine structure (EXAFS).<sup>148</sup> It was





**Fig. 5** Solubility of metal oxides in various DESs. (a) Solubility of metal oxides in maline (ChCl : malonic acid, 1 : 1), reline (ChCl : urea, 1 : 2), and ethaline (ChCl : ethylene glycol, 1 : 2) at 50 °C after 2 days. Reproduce with the data from ref. 116. Copyright © 2006, American Chemical Society. (b and c) Solubility of metal oxides in ChCl : ethylene glycol (EG) with either  $10^{-3}$  M trifluoromethanesulfonic acid (TFSA) or with lactic acid (LacA) at 50 °C after 2 days: (b) less soluble oxides, (c) more soluble oxides. Reprint with the permission from ref. 129. Copyright © 2020, Royal Society of Chemistry. (d) Solubility of metal oxides in *p*-toluenesulfonic acid monohydrate (PTSA) : chlorine chloride (ChCl) DESs at different HBD : HBA molar ratio at 50 °C. Reprint with permission from ref. 70, Copyright © 2019, American Chemical Society.

found that the high solubility of metals could be mainly attributed to metal complexation in DESs, where speciation has proven to be the key control factor. In diol-based DESs, the solvent anions (*i.e.*,  $\text{Cl}^-$ ), rather than solute anions, dominates the metal speciation. Metals in similar oxidation states form similar chlorine-based complexes. For instance,  $\text{Me}^{\text{I}}$  ions were found to form  $[\text{MeCl}_2]^-$  and  $[\text{MeCl}_3]^{2-}$  complexes, and  $\text{Me}^{\text{II}}$  ions form  $[\text{MeCl}_4]^{2-}$  complexes. A couple of exceptions were noted for  $\text{Ni}^{\text{II}}$ , with a unusual coordination by glycol molecules, and  $\text{Cr}^{\text{III}}$ , with a mixed chloro-aquo coordination. In reline, the metal coordination is dominated by chloride for the ions of the late transition metals (*e.g.*, Cu, Pd, Pt), while for the earlier transition metals such as Cr, Mn, Fe and Co, the first coordination consists of lighter atoms, *i.e.*, O or N originating from water or urea. Moreover, it was also reported that the substitution of alcohol group by thiol group could improve physical properties of ChCl-based DESs and improve solubilities of late transition metals like Cu and Zn, which could be attributed to the ligand structure and enhanced media acidity.<sup>151</sup> Recently, Pateli *et al.* (2020) demonstrated that the complexing abilities of the HBDs should have a larger contribution to the solubility of metals in DESs.<sup>129</sup> Their results showed that the strongly coordinating HBD with the effective chelating agent (*i.e.*, lactic acid (LacA)) exhibited 10 to 100 times higher solubility to most of the metal oxides compared to its counterpart with trifluoromethanesulfonic acid (TFSA), which only provided additional protons to the solution (as shown in Fig. 5b and c).<sup>129</sup>

On the other hand, the effect of different HBAs, such as ChCl, tetrabutylammonium chloride (tbaCl,  $[\text{N}_{4444}]\text{Cl}$ ), tetrabutylphosphonium chloride (tbpCl,  $[\text{P}_{4444}]\text{Cl}$ ), on the dissolution of metal oxides in DESs was also investigated.<sup>70</sup> For DESs with *p*-toluenesulfonic acid monohydrate (PTSA) as HBD, ChCl : PTSA was considered most appropriate for solubilization of metal oxides due to its best solution capacity, lower viscosity and broader thermal operation window. Besides, the HBD : HBA molar ratio also played a vital role in the solubility of metal oxides. As can be seen in Fig. 5d, the highest solubilities were not always obtained for the same molar ratio of PTSA : ChCl. For example, a higher HBA concentration could lead to higher solubilities for most metal oxides (including the metal oxides of Mn, Cu, Co, In and Pb), while the metal oxides of Fe and Zn showed higher solubilities in the more acidic DES with higher HBD concentration. Although research efforts are still required to further understand the mechanism behind, which should be related to both chemical and physical effects, it could be expected that selective metal recovery from complex matrices by DESs could be achievable *via* judicious choice of HBD, HBA and HBD : HBA molar ratio.

In addition, similar to some conventional metal leaching processes (*e.g.*, sequent extraction procedure for particulate trace metals<sup>152</sup> and dissolution of metals in spent nuclear fuel,<sup>153</sup> redox reactions may play important roles in the mechanisms of some metal recovery processes by DESs. Therefore, the reducibility/oxidizability is also known to control the dis-



solving capacity of DESs for metals. For example, the Co recovery from the  $\text{LiCoO}_2$  in the cathode of spent lithium-ion batteries LIBs relies on the reduction of  $\text{Co}^{3+}$  to  $\text{Co}^{2+}$ .<sup>154</sup> It showed that the temperature and duration of leaching Co from spent LIBs could be reduced to 180 °C and 12 h from 220 °C and 24 h (with the similar Co and Li extraction of >90%) by using reline, which had more negative reduction potential than ethaline. Note that the electrochemistry-based cyclic voltammetry (CV) method can be used to evaluate the reducing ability of DESs rapidly by the location of the reduction current peaks. As shown in Fig. 6a, the reduction peaks on the CV of ethaline at temperatures between 140 and 180 °C appeared from 0.40 to 0.50 V (vs. Ag), while those of reline shifted significantly to between -0.45 and -0.35 V (vs. Ag). Moreover, the diffusion of solutes and ions was the dominant transport process during leaching, and the structure of Co complexes was determined to be an octahedral molecular geometry  $\text{Co}(\text{urea})_2\text{Cl}_2$ . In addition to the reducibility of the DES, the presence of other reducing substances may also accelerate the leaching process. Peeters *et al.* (2020) found that metallic aluminum and copper in the LIBs could accelerate the leaching of cobalt by  $\text{ChCl}$ : citric acid DES.<sup>155</sup> The mechanism of the metal leaching process in DES can be described in Fig. 6. The crystal structure of  $\text{LiCoO}_2$  was attacked by protons of citric

acid and chloride anions of  $\text{ChCl}$ .  $\text{Co}(\text{III})$  was reduced to  $\text{Co}(\text{II})$ . Meanwhile, copper metal was oxidized to  $\text{Cu}(\text{I/II})$ , which could be reverted back to metallic Cu by metallic Al. Chloride anions stabilized Co by forming chloro-complexes, with tetrachlorocobaltate  $[\text{CoCl}_4]^{2-}$  being the predominant species.

#### 4.2. Influence of pH conditions of the original metal sources

Metal extraction by DESs is normally a pH-dependent process because this variable determines the species of metals and the ionization of the DES functional groups in different phases. Note that the pH in this section refers to the proton concentration in the original aqueous solutions containing metals, while the effect of the acidity of the DESs has been discussed previously. The influence of the pH of the original metal aqueous sources on the process performance is determined by the separation mechanism of the metals by DESs. For most type III DESs (mixtures of organic salts like quaternary ammonium salts and organic HBDs like carboxylic acids), the extraction of most metals (*e.g.*, Cu, Co, Zn, Fe, Cd, *etc.*) from aqueous solutions follows the mechanism of deprotonation of the HBDs (organic acid or alcohol) or the chelating agents followed by their complexation with the metal cations to form a charge-neutral complex.<sup>113,126,156–158</sup> In this case, metal extraction has a positive correlation with the pH of the original solutions, which can be attributed to the enhancement of the deprotonation process with the decrease of the proton concentration.<sup>113,126,157</sup> However, an excessive increase of pH would lead to the precipitation of the metal ions in the form of hydroxides, resulting in the reduced extraction efficiency at the high pH value (also refer to Fig. 7a).<sup>126,157</sup> Therefore, the optimized pH for metal extraction by DESs largely depends on the highest pH value to avoid the formation of the metal hydroxide precipitation, for example, 5.0–5.5 for Cu,<sup>113,158</sup> 8.0 for Zn,<sup>157</sup> and 7.0 for Cd.<sup>126</sup> In contrast, the extraction of some other metals like Pt and Pd by DESs could be improved in acidic solutions with low pH values.<sup>86,159</sup> Liu *et al.* (2021)<sup>159</sup> found that the extraction efficiency of Pt by H(D)ESs composed of TOPO and environmentally friendly organics (*i.e.*, menthol, butanol, hexanoic acid, *etc.*) gradually rise with the increasing HCl concentration in the aqueous solutions (as shown in Fig. 7b). These results were originated from the promoted protonation of TOPO and the improved ability to attract Pt(IV) in acidic media with strong ion strength of hydrogen.<sup>159</sup> Besides, the increasing concentration of  $\text{Cl}^-$  with the addition of HCl would cause the common-ion effect, which weakens the hydrolysis of  $\text{PtCl}_6^{2-}$  and enhance its combination with the extractant.<sup>160</sup> Tang *et al.* (2021)<sup>115</sup> also observed a similar declining trend of the extraction efficiency with the increase of aqueous pH when using the methyltrioctylammonium chloride ( $[\text{N}_{8881}]\text{Cl}$ ) and 1-hexanol/hexanoic acid-based DESs to extract Pd(II) from HCl aqueous solution (as shown in Fig. 7c). They also ascribed the deteriorated Pd(II) extraction performance to the decrease of non-hydrated  $\text{PdCl}_4^{2-}$  and the formation of hydrated  $[\text{PdCl}_3(\text{OH})]^{2-}$  in the solution with high pH, which enhanced the hydrophilicity of the Pd species and therefore reduced their partition into the hydrophobic DES phase.



**Fig. 6** The redox reactions in the DESs based metal recovery processes. (a) Cyclic voltammograms of  $\text{ChCl}$ : ethylene glycol (left) and  $\text{ChCl}$ : urea (right) DESs recorded at a fixed scan rate of  $50 \text{ mV s}^{-1}$ . Reprint with permission from ref. 154, Copyright © 2020, Royal Society of Chemistry. (b) Schematic diagram of cobalt recovery from lithium-ion battery cathode materials using  $\text{ChCl}$ : citric acid DES with the acceleration of aluminum and copper metal. Reprint with permission from ref. 155, Copyright © 2020, Royal Society of Chemistry.







**Fig. 7** The effects of pH on the performance of metal extraction by DESs. (a) The effect of pH on Zn-ion extraction by choline chloride-phenol (1 : 2) DES with 8-hydroxy quinoline as a chelating agent. Reprint with permission from ref. 157, Copyright © 2021, Elsevier B.V. (b) The effects of the concentration of HCl on the Pt(IV) extraction by the trioctylphosphine oxide (TOPO)-based DESs. Reprint with permission from ref. 159, Copyright © 2021, Elsevier B.V. (c) The effects of pH on the Pd(II) extraction by the methyltriethylammonium chloride ([N<sub>8881</sub>]Cl)-based DESs. Reprint with permission from ref. 115, Copyright © 2021, Elsevier B.V.

### 4.3. DES extraction-based hybrid process for metal recovery

#### 4.3.1. Integrated DES extraction and precipitation process.

Integrated DES extraction and precipitation process has been widely employed for metal recovery like Co, In, Sn, *etc.* This concept involves metals being dissolved first in DES and then selectively recovered through subsequent precipitation.

Co recovery from spent LIBs is one example. In the study by Tran *et al.* (2019),<sup>98</sup> LiCoO<sub>2</sub> was dissolved in ChCl:EG (1 : 2) through simultaneous oxidation of EG and reduction of cobalt at 220 °C and duration of 24 h. In the precipitation process, a mixture of CoCO<sub>3</sub>, Co(OH)<sub>2</sub>, and Co<sub>3</sub>O<sub>4</sub> was obtained with the addition of Na<sub>2</sub>CO<sub>3</sub> solution. About 74% of the cobalt could be

recovered as Co<sub>3</sub>O<sub>4</sub> after calcination at 500 °C for 6 h, which was useful in the creation of new LIBs (see the schematic diagram in Fig. 8a). Moreover, it was reported in the following studies that the selection of the precipitants could have effects on the properties of the recovered metal compounds. For example, Roldán-Ruiz *et al.* (2020) used an integrated PTSA-based DES extraction and precipitation process for Co recycle from LIBs showing that LiCoO<sub>2</sub> could be sufficiently dissolved in these solvents at 90 °C only after 15 min, and 94% of cobalt could be recovered in the form of Co<sub>3</sub>O<sub>4</sub> through subsequent precipitation with Na<sub>2</sub>CO<sub>3</sub> or (NH<sub>4</sub>)<sub>2</sub>CO<sub>3</sub> and final calcination.<sup>97</sup> But they found that the precipitated solids generated by Na<sub>2</sub>CO<sub>3</sub> precipitant exhibited poorly crystalline XRD pattern that could barely be assigned to Co(CO<sub>3</sub>)<sub>0.5</sub>(OH)<sub>0.11</sub>·H<sub>2</sub>O (JCPDS card no. 00-0048-0083), while the precipitate obtained upon the addition of the (NH<sub>4</sub>)<sub>2</sub>CO<sub>3</sub> precipitant had enhanced crystalline features that allowed confident assignment to Co(CO<sub>3</sub>)<sub>0.5</sub>(OH)<sub>0.11</sub>·H<sub>2</sub>O (see Fig. 8b). Similar results were reported by a study conducted by Wang *et al.* (2020),<sup>154</sup> in which around 95% of Co in the spent LIBs could be extracted by reline at 180 °C. The cobalt in solution could be recycled as a cubic cobalt oxide spinel (Co<sub>3</sub>O<sub>4</sub>) through a consecutive dilution-precipitation-calcination process, and H<sub>2</sub>C<sub>2</sub>O<sub>4</sub> and NaOH were proposed to be a preferred precipitant than Na<sub>2</sub>CO<sub>3</sub> due to the better crystallinity of calcined powder (see the comparison of XRD and XPS results in Fig. 8c) and less Na in the hydrated cobaltous carbonate.

Besides, different target metals can be obtained separately by the multi-step precipitation procedure. Zürner and Frisch (2019) leached In and Sn from zinc flue dust using oxalate and selectively separated Zn and Fe from the leaching solution *via* two subsequent precipitation steps, leaving the target metals In and Sn in solution (see Fig. 8a).<sup>161</sup> The leaching yield (the ratio of the amount of the respective metal detected in the leachate to that in the dried flue dust) of In and Sn could reach up to 100% in oxalate at 70 °C after 24 h, while large amounts of Zn and Fe (leaching yield also reaching 90 to 100%) were leached together. In order to separate the main flue dust components (Zn and Fe) from In and Sn, the oxalate leachate was first diluted 1 : 10 with deionized water resulting in 95% of zinc (with respect to the amount in the original flue dust) precipitated in the white precipitant which was composed of 90% ZnC<sub>2</sub>O<sub>4</sub>·2H<sub>2</sub>O, 3.6% PbC<sub>2</sub>O<sub>4</sub> and small amounts of Fe, Mn, Cu (all below 1%) (as shown in Fig. 8b). Afterward, iron oxalate complexes in the diluted oxalate leachate were reduced by photolysis and precipitated as FeC<sub>2</sub>O<sub>4</sub>·2H<sub>2</sub>O (see reaction formulations and image in Fig. 8c). Meanwhile, indium and tin were not detectable in all the precipitates, remaining in the solution for further recycling.

However, it should be noted that most of the DESs could not be regenerated and reused for the next metal extraction cycle after separating the metals by the precipitation process. This is because integrating DES extraction with the precipitation process cannot avoid a series of physical and chemical procedures, including dilution, pH adjustment, redox reactions, as well as successive addition of various precipitants, which would change the composition (*e.g.*, by diluting and





**Fig. 8** (a) Schematic diagram of cobalt recovery from LIBs using DESs. Reproduced based on ref. 98, Copyright © 2019, Springer Nature Limited. (b) Comparison of the XRD patterns of the precipitate obtained upon addition of  $\text{Na}_2\text{CO}_3$  (left) or  $(\text{NH}_4)_2\text{CO}_3$  (right) to the Co-loaded DES after extraction from spent LIBs. Reprint with permission from ref. 97. Copyright © 2020, American Chemical Society. (c) XRD patterns (left) and XPS spectra (right) of the calcined powder after the precipitation process by  $\text{H}_2\text{C}_2\text{O}_4$ ,  $\text{Na}_2\text{CO}_3$ , or  $\text{NaOH}$ . Reprint with permission from ref. 154. Copyright © 2020, Royal Society of Chemistry.

coprecipitating the main components) or even destroy the structure (*e.g.*, by chemical reactions) of DESs.<sup>154,161–163</sup> This issue along with the relatively complex procedures of the precipitation processes may hinder the industrialization of the DES-based metal recovery process. Regarding this, more sustainable and convenient DES-based metal extraction processes integrated with precipitation were developed in recent studies. Liu *et al.* (2020) used the DES composed of guanidine hydrochloride (GUC) and lactic acid (LAC) with a molar ratio of 1 : 2 to selectively leach neodymium (Nd) from end-of-life NdFeB permanent magnets by one dissolution step, which could achieve more than 90% dissolution ratio of Nd and a high separation factor (>1300) between Nd and Fe at 40 °C for 6 h.<sup>130</sup> The Nd dissolved in the GUC:LAC DES could be stripped simply by adding solid oxalic acid to yield an  $\text{Nd}_2(\text{C}_2\text{O}_4)_3$  pre-

cipitate, which was further calcinated to prepare the  $\text{Nd}_2\text{O}_3$  product with Nd purity of 99.56% and total recovery rate of Nd of 83.1% in the whole process. The GUC-LAC DES could be reused for the next selective leaching cycle and the same dissolution property and chemical stability of the DES could be retained after 3 cycles (see Fig. 9b). Lu *et al.* (2021) proposed a convenient one-pot extraction process using a ChCl:oxalic acid DES (1 : 1) to extract both Li and Co from  $\text{LiCoO}_2$  at 90 °C for 2 h with extraction efficiencies of around 80–90%.<sup>163</sup> Notably, the separation of Li and Co from the DES liquid phase in the form of oxalate precipitates could be attained only upon cooling down the Li and Co-loaded DES leachate without the addition of any precipitant. The Li and Co products were further separated as  $\text{LiHC}_2\text{O}_4 \cdot 4\text{H}_2\text{O}$  and  $\text{CoC}_2\text{O}_4 \cdot 2\text{H}_2\text{O}$  with high purity of 99% and 98%, respectively, by repeating water



washing according to the difference in their solubility. They further reported that oxaline could retain its structure after the extraction process at 90 °C and could be reused for at least another 4 cycles with nearly unchanged extraction efficiencies of Li (80–90%) and slightly declined extraction efficiencies of Co (around 75%) (see Fig. 9c). But here, we need to highlight that the content of oxalate anions ( $C_2O_4^{2-}$ ) in the DES should be reduced with the cyclic operation of metal extraction due to the precipitation of the Li and Co oxalate. Thus, the ChCl:oxalic acid DES cannot be reused for many cycles in this case.

Despite the aforementioned research efforts, the sustainability (*i.e.*, the recyclability of the DESs) and ease of operation of the DES-based metal extraction processes integrated with precipitation should be further investigated and improved in future studies.

**4.3.2. Integrated DES extraction and electro-deposition process.** DESs have also been proposed as emerging electrolytes with several advantages, including less acidic formulation, improved surface finish on cast pieces, and improved current efficiency, over conventional electrolytes (*e.g.*, concentrated phosphoric acid sulfuric acid mixtures).<sup>33</sup> Integrated DES extraction and electro-deposition process has been regarded as a promising method for metal recovery with the advantage of the high solubility of metal salts, which would allow both selective dissolution and subsequent electro-deposition of metals. Additionally, modulating the deposition process is possible with DESs as electrolytes, particularly owing to the tenability of these solvents by changing the HBA, the HBD or their molar ratio. Compared with other recycling methods like hydrometallurgy and pyrometallurgy, integrated DES extraction and electro-deposition process has the advantages of high purity deposits, easy operation and potentially lower costs.<sup>164</sup>

Several studies have reported metal recovery through DES-based extraction integrated with the electro-deposition process. The electro-deposition process allows the direct transition of the target metals from the oxide or complex state in the DESs to the metallic state on the solid electrodes with high purity, which greatly facilitates the practical application of the recovered metals. For instance, Poll *et al.* (2016) proposed a method for recycling lead from Pb-based hybrid organic–inorganic perovskite (HOIP) photovoltaic devices by simultaneous dissolution and electro-deposition using ethaline, which is summarized in Fig. 10.<sup>165</sup> Pb in HOIP was dissolved in the DES as  $[PbCl_3]^-$  due to atomic solvation of Cl. Subsequently, up to 99.8% of Pb in HOIP could be extracted using a Pb working electrode, which was ready for industrial applications without further purification. Ru *et al.* (2016)<sup>167</sup> further investigated the dissolution–electrodeposition pathway of PbO in ethaline and found that direct deoxidation of PbO to metallic Pb and the dissolution–electrodeposition took place simultaneously.  $[PbO-Cl-EG]^-$  was formed during the dissolution process, and subsequently reduced and deposited on Cu substrate. Additionally, the metallic Pb deposited from  $[PbO-Cl-EG]^-$  was proposed to act as nucleation centers for the growth of subsequently generated Pb.<sup>167</sup> In addition, Zn from

cupola furnace dust was also successfully recovered through dissolution and electrodeposition in a ternary DES consisting of ChCl:urea:EG (1:0.5:0.5).<sup>119</sup> Specifically, about 38% of Zn in cupola furnace dust could be dissolved in the DES at the temperature of 60 °C and duration of 48 h, and highly pure metallic Zn with fine and smooth morphology was electrodeposited with moderate reductive potentials. Meanwhile, the Fe-rich dust residue with lower Zn content can be recycled in cupola furnace or in other iron/steel-making processes. In the study by Tran *et al.* (2019),<sup>98</sup> the recovery of Co from spent LIBs dissolved in ethaline was also attempted by the electro-deposition process. It showed that Co in DES could be electrodeposited on a stainless steel mesh working electrode as Co(OH)<sub>2</sub>. More importantly, although metal separated from DES by electro-deposition was energy-intensive compared to the chemical precipitation, such procedures could regenerate the DES (resulting DES turned bluish-green again), which could leach a comparable amount of Co as the original one, indicating that the DES itself could be recycled for additional cycles of metal extraction (as shown in Fig. 10b).

Furthermore, the structure and morphology of the metal recovered by the electrodeposition in DESs are associated with the selections of DESs composition, the substrates and applied overpotential. For example, different morphologies of Pb deposit could be obtained with different  $[PbCl_3]^-$  concentrations in DES.<sup>164</sup> The growth layer of Pb deposit was turned away from center type towards the edge and corner types with the increase of  $[PbCl_3]^-$  concentration (see Fig. 10c). Sebastian *et al.* (2018) systematically investigated the structure and morphology of nickel electro-deposition in reline.<sup>166</sup> They reported that the Ni electrodeposited in reline favored the morphology of rounded nanoclusters, resulting from the high viscosity of the medium and the strong interaction between the species of the DES with precursor and substrate. Smaller Ni clusters were observed on the platinum substrate compared with the glassy carbon substrate, which could be attributed to the lower surface diffusion on platinum. Furthermore, using high applied overpotential could obtain similar-size and homogeneous Ni nanoparticles with circular-shape holes (possibly related with the formation of hydrogen bubbles during deposition). In comparison, at low applied overpotential, the Ni nanoparticles moved and formed triangular arrays with minimized holes due to the suppression of the hydrogen formation reaction on the platinum substrate (Fig. 10d).

## 5. Current applications of DES for metal recovery and separation from different matrices

To date, DESs have been applied or investigated in a variety of scenarios for metal extraction. This section is dedicated to summarizing the current progress of the applications of DESs for metal extraction and evaluating the performance that DESs offer (Fig. 11).



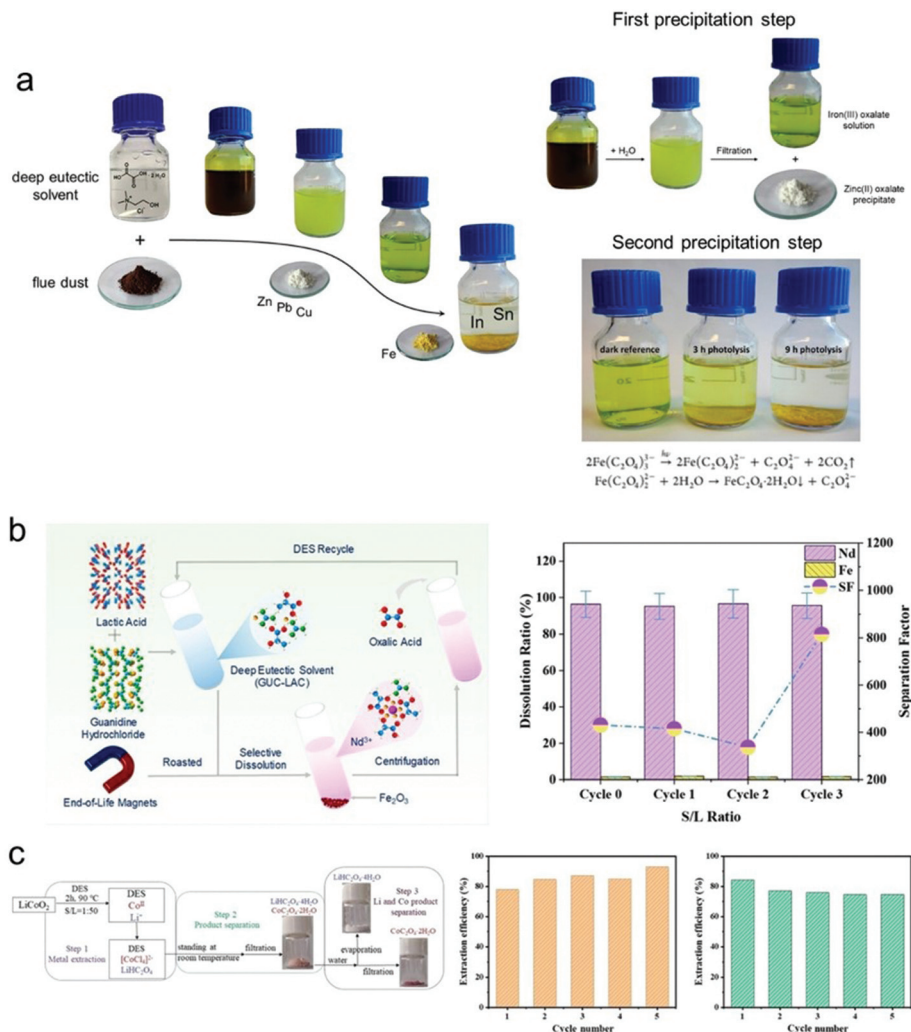


**Fig. 9** (a) Schematic diagram of leaching and selective extraction of zinc, iron, indium, and tin using ChCl:oxalic acid DES-based two-step precipitation procedure (left); dilution of oxaline leachate and precipitation of white zinc oxalate next to the green-colored filtrate in the first precipitation step (upper right); photograph and reaction formulations of photolysis of iron(III) oxalate solution using a UV lamp in the second precipitation step (lower right). Reprint with permission from ref. 161. Copyright © 2019, American Chemical Society. (b) Schematic diagram of selectively leaching neodymium from end-of-life NdFeB permanent magnets by guanidine hydrochloride:lactic acid DES (left) and the recycling performance of the DES (right). Reprint with permission from ref. 130. Copyright © 2020, American Chemical Society. (c) Schematic diagram of the one-pot extraction process using ChCl:oxalic acid DES for the recovery of lithium and cobalt from LiCo<sub>2</sub> and the recycling performance of DES for Li extraction (middle) and Co extraction (right). Reprint with permission from ref. 163. Copyright © 2021, American Chemical Society.

## 5.1 Studies in model systems

Since the applications of DESs in metal recovery and separation are still in their infancy, the studies carried out in model systems are advantageous to investigate the mechanisms and evaluate the validation of the DESs-based metal separation process. This is the case of separations from pure aqueous solutions containing only certain target metal salts.

Type III DESs, which are composed of organic salts (*e.g.*, any type of phosphonium, sulfonium, ammonium, *etc.*) as HBAs and organic HBDs (*e.g.*, amides, carboxylic acids and alcohols), have been reported to achieve efficient extraction of various metals, including Au(III), Pd(II), Fe(III), Co(II), Mn(II), *etc.*, from model aqueous systems.<sup>115,168,169</sup> For example, Au(III)

in the aqueous solution could be extracted by the H(D)ESs based on quaternary ammonium salts (*i.e.*, [N<sub>8881</sub>]Br as HBA and *n*-hexanoic acid as HBD) with a high extraction efficiency (>90%) as well as high selectivity against other metal impurities (*i.e.*, Mg(II), Al(III), Mn(II), Co(II), Cu(II), Ce(III) and Ni(II)).<sup>114</sup> Subsequently, the extracted Au in the DESs phase was easily and completely stripped by NaBH<sub>4</sub>. Tang *et al.* (2021)<sup>115</sup> reported that the [N<sub>8881</sub>]Cl-based DESs with various fatty alcohols or acids (*e.g.*, EG, Gly, 1-hexanol, propionic acid, and hexanoic acid) could also selectively extract Pd(II) from the HCl aqueous solutions with extremely high extraction percentage. Since most of the reported extraction percentages are higher than 99% in this study, the potential of excellent extraction performance of quaternary ammonium-based DESs for Pd





**Fig. 10** (a) Schematic diagram of the DES-based electro-deposition process for lead recovery from hybrid organic–inorganic perovskite (HOIP) material. Reprint with the permission from ref. 165. Copyright © 2016, Royal Society of Chemistry. (b) Recyclability of the DES after electro-deposition process.  $\text{LiCoO}_2$  (LCO) was first added to the pure DES. Then, after stirring under 135 °C heat, cobalt was leached into the solution, causing the color change from clear to green (first to second photograph). The  $\text{Co}_2^+$  ions were electrodeposited onto a substrate, allowing the remaining DES to be recovered (third photograph). LCO was added to the recovered DES for another cycle of electrodeposition and resulted in a similar color change and leaching efficiency to the first cycle (last photograph). Reprint based on ref. 98, Copyright © 2019, Springer Nature Limited. (c) SEM images of lead powders electrodeposited in a DES at cell voltage 2.5 V and 243 K for 2 h with different  $[\text{PbCl}_3]^-$  concentrations: 10 mM (left), 20 mM (middle), and 40 mM (right). Reproduced based on ref. 164, Copyright © 2015, Elsevier B.V. (d) Schematic representation of Ni(II) electro-deposition in DES on Pt (111) and atomic force microscopy image ( $2 \times 2 \mu\text{m}^2$ ) of the Ni clusters. Reprint with the permission from ref. 166. Copyright © 2018, American Chemical Society.

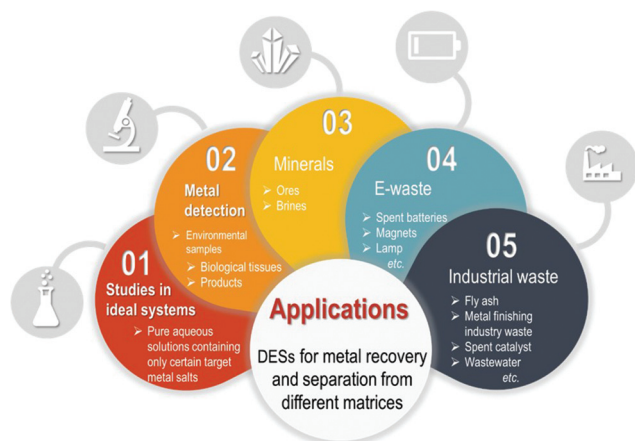


**Fig. 11** Various applications of DESs for metal separation and recovery from different matrices.

extraction is worth further investigation. In a recent study, H(D)ES composed of Aliquat 336 (the main active substance is  $[\text{N}_{8881}]\text{Cl}$ ) and *l*-menthol with the molar ratio of 3 : 7 was investigated for Li(I), Co(II), Ni(II), Mn(II), and Fe(III) separation from

the model aqueous systems.<sup>169</sup> High extraction percentages of >99% for Fe(III), Mn(II) and Co(II) were achieved through a multi-metal separation procedure, with 1 mol L<sup>-1</sup> HCl, 3 mol L<sup>-1</sup> HCl, and 5 mol L<sup>-1</sup> LiCl added into the mixed-metal solution in sequence and Aliquat 336: *l*-menthol H(D)ES as the extractant. The solvation mechanism of the metal ions in the type III DESs with high ionic strengths involved an anion exchange reaction where the metal ions form a complex with the halide ions (*e.g.*, in the form of  $\text{MeCl}_4^{(n-)}$ ), which would electrostatically interact with the quaternary ammonium cations (*e.g.*,  $[\text{N}_{8881}^+]$ ,  $[\text{Ch}^+]$ ) in the DESs.<sup>115,168–170</sup> Take  $[\text{N}_{8881}]\text{Cl}$ :*l*-menthol H(D)ES as an example, the anion exchange mechanism for metal extraction can be given as:



where  $\text{R}' = \text{CH}_3$ ,  $\text{R} = \text{C}_8\text{H}_{17}$ .

Furthermore, some studies have endeavored to reveal the mechanism of metal distribution between ionic DESs and conventional organic solvents in model systems, which improved the understanding of the behaviors of metals and equilibrium



of various metal complexes in the DESs-involving system. For example, Foreman (2016) investigated the solvent extraction of metals from the DESs formed from  $\text{ChCl}$  (e.g.,  $\text{ChCl}$ :glycolic acid) by conventional solvent extraction reagents, such as lipophilic chloride IL (Aliquat 336) and di-(2-ethylhexyl) hydrogen phosphate (DEHPA) diluted with hydrocarbons, in the model systemsto evaluate the application potential of the DESs-based metal extraction process.<sup>95</sup> It was shown that zinc (Zn), cadmium (Cd) and some transition metals such as Co, Cu and Fe could be extracted from the DES into the organic layer. However, when chloride IL (i.e., Aliquat 336) was used as an organic solvent to extract metals from  $\text{ChCl}$ :lactic acid DES, the lactate anions would accumulate in the DES layer and it would be gradually converted to choline lactate with the reuse of the DES phase, which suppressed the extraction of some metals (e.g., Co and Ni) by forming unextractable complexes.<sup>171</sup> To improve the reusability of the DES, a new solvent extraction system for recovery of both Co and Ni from  $\text{ChCl}$ -based DES using a combination of DEHPA and a pyridyl pyrazole in solvent 70 was proposed in the following study, which could prevent the accumulation of lactate in the DES phase and was regarded as a less harmful alternative due to its low concentration of aromatic compounds to the Aliquat 336 in the aromatic diluent.<sup>171</sup> Besides, it was found in their experiments that the distribution ratios of metals (which refers to the ratio of the total concentration of metal in organic layer to the total concentration of metal in denser layer (i.e., DES

layer)) could be varied with the water content of the DES phase (as shown in Fig. 12a).<sup>95</sup> To further reveal the mechanism behind the solvent extraction of metals in the DES system, Foreman *et al.* developed a chemical model based on the distribution of several representative metals (including Cd, Co, Ga, In, Pd, Re, and Zn) in the model solvent extraction systems involving wet DES (mixture of  $\text{ChCl}$ :lactic acid DES and aqueous sodium chloride) and conventional organic solvents, such as Aliquat 336, Cyanex 301 (mainly composed of bis (2,4,4-trimethylpentyl)dithiophosphinic acid) and Cyanex 923 (a mixture of trialkylphosphine oxides including trioctylphosphine oxide (TOPO)).<sup>172</sup> Introducing the activity coefficient concept, they attributed the lower distribution ratios of most metals in organic phase with the decrease of water content in DES phase to the increased activity coefficient of the chloride anions. The increased activity coefficient of chloride anions in DES phase with lower water content could result in the greater competition abilities of chloride anions against the anionic complexes from the organic phase to form the unextractable metal-chloride complexes, and remain in the DES phase.<sup>172</sup> More recently, Foreman and co-workers performed the solvent extraction of a selection of metals (e.g., Au, Pd, Tc, In and Re) in mixtures of a chloride rich DES (i.e.,  $\text{ChCl}$ :EG) with aqueous salt solutions to further created a mathematical model using the activity coefficient/function equation (specific ion interaction theory).<sup>168</sup> This new model was able to describe and explain the activity function of ions in chloride rich DESs,



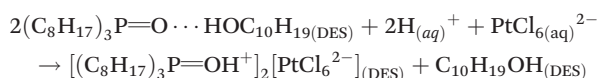
**Fig. 12** The metal extraction from DESs by conventional solvent extraction organic reagents in model systems. (a) The relationship between the water content of the DES phase and the distribution ratios for cadmium, cobalt, copper, iron, manganese and zinc for extraction from the DESs into a conventional organic solution of Aliquat 336. Reprint with permission from ref. 95. Copyright © 2016 The Author(s). (b–d) the agreement between the theoretically predicted (by the mathematical model using the activity coefficient/function equation with specific ion interaction theory) and experimentally measured distribution ratios of (b) gold, (c) rhenium, and (d) palladium. A model which is perfectly able to predict the distribution ratios would create a straight line of points that would obey the equation  $y = x$  where  $x$  is the predicted distribution ratio and  $y$  is the measured distribution ratio. Reprint with permission from ref. 168. Copyright © 2020, Royal Society of Chemistry.



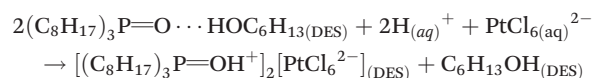
suggesting its potential for the predictions of the behavior of a solvent extraction system where one of the liquid phases is a mixture of DESs and aqueous salts (see Fig. 12b–d).

Additionally, non-ionic type V DESs have been also studied to extract metals from aqueous solutions. Some typical type V DESs, including menthol-based, thymol-based and trioctylphosphine oxide (TOPO)-based DESs, were reported to be capable of selective metal extraction, such as In(III), Pt(IV), Pd(II), Fe(III), Cu(II) or Co(II), in the model systems of synthetic aqueous solutions.<sup>86,90,113,159,173</sup> For example, Schaeffer *et al.* (2020)<sup>86</sup> reported that the TOPO-based DESs displayed good selectivity towards Pt<sup>4+</sup>, Pd<sup>2+</sup>, and Fe<sup>3+</sup> over other transition metals (*i.e.*, Cu<sup>2+</sup>, Co<sup>2+</sup>, Ni<sup>2+</sup>, and Cr<sup>3+</sup>) in HCl aqueous solution; the selective separation of Pt(IV) from Pd(II) in HCl solutions could be also achieved by using the TOPO-based DESs extractants (*i.e.*, TOPO: decanoic acid).<sup>173</sup> The extraction and separation of Cu(II) from other transition metals like Co(II) and Ni(II) could use the type V DESs based on menthol or its aromatic counterpart thymol combined with long-chain carboxylic acids.<sup>113</sup> It was shown that the selectivity of the metal extracted by type V DESs could be tuned by the selection of the DESs components, the mole fraction of the components, and the operating conditions during the solvent extraction process (*e.g.*, pH, salinity, temperature, *etc.*).<sup>113,159,173</sup> Besides, the mechanical studies of the non-ionic type V DESs for metal extraction could be easier in the model systems. Take TOPO-based H(D)ESs for Pt(IV) extraction as an example, TOPO: 1-menthol, TOPO: 1-hexanol, and TOPO: 1-butanol were selected to investigate the interaction between H(D)ESs and PtCl<sub>6</sub><sup>2-</sup> in a model system which was prepared by dissolving H<sub>2</sub>PtCl<sub>6</sub> in distilled water with hydrochloric acid.<sup>159</sup> Because of the relatively simple compositions of the model system, the status and structure of PtCl<sub>6</sub><sup>2-</sup> and H(D)ESs before and after extraction could be well characterized by UV-Vis and FT-IR spectra, which indicated that the status of PtCl<sub>6</sub><sup>2-</sup> were maintained throughout the extraction process and the positive charge of the DESs phase during the extraction process originated from the protonation of phosphorus–oxygen double bond (P=O) in TOPO. Accordingly, the mechanisms of the TOPO-based H(D)ESs for Pt(IV) extraction can be summarized as ion-association and the reaction formulations as follows:

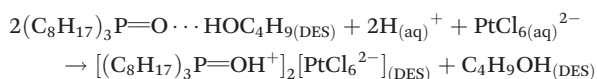
TOPO: 1-menthol:



TOPO: 1-hexanol:



TOPO: 1-butanol:



On the other hand, due to the electrically conductive properties of the DESs, another main application of DESs is to

incorporate metal ions into DESs for electrodeposition. The ionic type III DESs composed of ChCl as HBAs were extensively investigated as the green organic electrolytes for metal electrodeposition in model systems.<sup>85,109,174</sup> Ethaline was well suited for recovering metallic elements from metal oxides, including MnO<sub>2</sub>, MnO, Fe<sub>2</sub>O<sub>3</sub>, Fe<sub>3</sub>O<sub>4</sub>, Co<sub>3</sub>O<sub>4</sub>, CoO, NiO, CuO, Cu<sub>2</sub>O, ZnO and PbO, through electro-oxidation accompanied by subsequent electro-reduction of the liberated metal ions.<sup>109</sup> Electrodeposition of Pd–Pt–Ag ternary-alloy films was achieved in reline (molar ratio of 1:2) electrolyte containing sulfosalicylic acid dihydrate as organic additive at 70 °C.<sup>174</sup> Ethaline and reline were applied for the electrodeposition of Zn–Sn alloys, the morphology and composition of which could be changed by the selection of the DESs.<sup>175</sup> The selection of the HBDs of the DESs was also critical to determine selectivity for extracting certain metals. For example, Landa-Castro *et al.* (2020)<sup>176</sup> compared the performance of reline, glyceline and ethaline for electrodeposition of Ni–Co alloy, and reline rendered the best results to attaining up to 83.6% of nickel leaching and 53.3% of cobalt after 24 h.

In general, the studies carried out in the model aqueous systems demonstrate the great application potential of DESs for metal extraction because of their high extraction efficiency, high selectivity, as well as environmental friendliness. More specifically, adjusting the compositions of DESs can effectively tune the selectivity towards a variety of target metals and improve the efficiency of the metal extraction. These results have attracted increasing interest in recent years and led to more and more investigations in metal extraction by DESs from different matrices, which are discussed in the following sections.

## 5.2 Metal detection in environmental samples, biological tissues, food and cosmetics

The accurate determination of the metal elements in environmental samples (*e.g.*, water and soil samples), biological tissues and products (*e.g.*, food, cosmetics and personal care products), is critical to evaluate their impacts on the environment and human health, and thus, is receiving increasing attention in last decades.<sup>177</sup> However, the direct instrumental measurement of metal ions at trace level is limited by their ultra-low concentrations (*i.e.*, μg or even ng per kg sample) as well as the complex components such as a variety of co-existing ions and high concentration of other species in the real samples. Therefore, separation and preconcentration methods are often required prior to the instrumental analysis to selectively extract and concentrate the trace metal ions from various real samples or complex matrices.<sup>178</sup> Techniques like inductively coupled plasma-optical emission spectrometry (ICP-OES), graphite furnace atomic absorption spectrometry (GF-AAS) and flame atomic absorption spectrometry (FAAS) have benefited from such preconcentration methods.<sup>179,180</sup> Until recently, the separation and preconcentration methods reported in literature generally include liquid–liquid extraction (LLE),<sup>181</sup> coprecipitation,<sup>180,182</sup> liquid phase microextraction (LPME),<sup>179,183</sup> solid phase extraction (SPE),<sup>184</sup> solid phase



microextraction (SPME).<sup>185,186</sup> In addition, microwave-assisted acid digestion<sup>187,188</sup> and ultrasound-assisted extraction<sup>178,189</sup> were developed and used to improve the extraction efficiencies of metals from samples. Although most of these sample preparation methods can fulfill the technical requirements for the subsequent instrumental analysis, the use of harmful organic solvents, strong mineral acids and oxidizing reagents is still a difficult challenge to tackle.<sup>178,179</sup> Recently, research efforts are dedicated to developing more eco-friendly sample preparation methods for simple, cost-effective, rapid, sensitive and accurate metal analysis.<sup>177</sup> In these regards, DES-based metal extraction methods have attracted increasing interest due to their enhanced environmental, health and safety profile with respect to classic solvents as well as their application in metal oxide extraction, nanoparticles synthesis, drug dissolution, and carbon dioxide absorption.<sup>179,181</sup> DESs-based sample preparation methods for the determination of metal in environmental samples, biological tissues, food and cosmetics are introduced in this section and summarized in Table 4.

As seen in Table 4, diverse trace metals, including Ag(I),<sup>22</sup> Cr(III),<sup>179,190</sup> Co(II),<sup>191</sup> Ni(II),<sup>177,191</sup> Cu(II),<sup>192</sup> Fe(III),<sup>178</sup> Zn(II),<sup>157</sup> etc., in real water samples (e.g., wastewater, seawater, mineral water and well water, etc.), biological tissues (e.g., fish muscle and liver, macroalgae, blood, leaves and roots, etc.), food (e.g., vegetables, milk, wine, etc.) and cosmetics (e.g., lipsticks, eye shadows, etc.) could be successfully extracted and concentrated by DESs prepared with different components according to the properties of the target metals. The most commonly studied DES-based LPME method for metal detection can be conducted in four steps as illustrated in Fig. 13.<sup>177,190,193</sup> Briefly, in the first step the analyte sample is first adjusted to the desired pH; in the second step complexing agent and DES are added into the analyte solution and mixed uniformly by vortexing or ultrasonication under optimal temperature; in the third step the metal-ion-containing DES-rich phase is separated from the initial solution by centrifugation; in the fourth step the concentration of metal ions is determined by the following instrumental analysis.

In addition, DESs could be used to modify the solid materials, such as cotton<sup>194</sup> and graphene oxide (GO),<sup>22</sup> to prepare the functionalized sorbents for SPE of metals. The procedure of SPE can be briefly described as:<sup>22,194</sup> (1) preparation of the DESs modified sorbents; (2) pH adjustment of the sample solution; (3) adsorption of the analytes by either mixing the tested solution with the solid sorbents or passing the solution through the microcolumn made by the sorbents; (4) desorption of analyte from the sorbents and quantification by instrument.

The validation of the methods of metal analysis often follows the international guidelines described under the ISO/IEC 17025:2005 protocol.<sup>158,193</sup> As reported in Table 4, most DES-based metal determination methods exhibit low limit of detection (LOD) and limit of quantification (LOQ), large pre-concentration factor (PF), small relative standard deviation (RSD < 5%) and high percentage recoveries (>90%). This indicates that high sensitivity, good reproducibility and high accu-

racy of metal detection are achieved using DESs as alternative solvents. Here, it must be noted that the LODs and LOQs of these metal determination methods are determined by both the DES-based metal extraction/separation process and the followed instrumental analysis. Furthermore, the results of these investigations also showed that commonly existing ions, including alkaline and alkali earth ions such as Na<sup>+</sup>, K<sup>+</sup>, Mg<sup>2+</sup>, and Ca<sup>2+</sup> Al<sup>3+</sup> had negligibly adverse effects on the extraction of metals by DESs.<sup>177,179,191</sup> Some studies also reported that the extraction time with the DES-based methods could be reduced to less than one hour or even to as short as 10 minutes.<sup>126,188,195</sup> The efficient metal extraction by DESs was also applied to remove heavy metals from biological tissues, and the ChCl-organic acids DES showed good removal effect on heavy metals, including Pb, Cd, As and Cu, from *Porphyra haitanensis* (a species of red algae).<sup>196</sup> In general, the developed DES-based metal extraction and preconcentration methods provide a sustainable, low-toxic, inexpensive, quick, sensitive, accurate, and efficient alternative to the conventional organic solvent extraction technique for metal determination from water, soil, biological tissues, food, and personal care products.

### 5.3 Minerals

The current global production of metals from minerals, such as ores and brines, is generally based on the smelting/leaching process at high temperatures, or the dissolution and extraction process using large quantities of strong acids/bases or organic solvents. Both of them require high energy costs and often generate various forms of wastes in gaseous, liquid or solid form with concerning degrees of negative environmental impacts.<sup>202</sup> Hence, mining industries have dedicated resources to develop novel environmentally benign approaches for metal extraction without sacrificing cost-effectiveness and competitiveness.<sup>91</sup> Recently, DESs have been investigated as a green alternative replacement to the toxic organic solvents for metal recovery from minerals owing to their comparable cost with the conventional solvents, high biodegradability and low toxicity.<sup>91,117</sup>

Entezari-Zarandi *et al.* (2019) assessed the dissolution of rare earth metals (Y, La, Ce, Nd and Sm), which are of importance in high-tech industries (e.g., catalytic, electrical and magnetic industries), from bastnasite ores in several ChCl-based DESs with urea, malonic acid, citric acid or binary mixtures thereof.<sup>91</sup> The solvometallurgical processes using ChCl-based DESs exhibited highly selective dissolution of the higher-atomic-number rare earth elements (e.g., Y, Nd and Sm) over their lower-atomic-number counterparts (e.g., La and Ce), as well as the marginal dissolution of the metal impurities (e.g., Ca, Mg and Fe) in the minerals. Moreover, their results indicated that the ChCl-based DESs with malonic acid or malonic acid + urea mixture as HBD had a higher affinity to dissolved rare earth metals compared to those with urea or citric acid + urea as HBD. Precious metal minerals, such as electrum (containing As and Ag), galena (containing Pb and Ag), chalcocopyrite (containing Cu and Fe), as well as tellurobismuthite







Table 4 Performance of DES-based methods used in metal detection from real water, biological tissues, food and cosmetic samples

Sample category	Separation & preconcentration method	Detection technique	Metal	DESS (HBA+HBD, molar ratio)	pH/Temp	Complexing agent	LOD	LOQ	PF/EF	RSD, %	Linear range	Sample details	Recoveries	Ref.
Biological tissue	UA-LPME	FAAS	Zn	ChCl: phenol (1:2)	8.0/60 °C	10 mg L <sup>-1</sup> 8-hydroxy quinoline	0.041 µg kg <sup>-1</sup>	0.136 µg kg <sup>-1</sup>	25	1.7%	0.25–15.0 µg kg <sup>-1</sup>	Fish and eel samples	92.8–101.3%	157
Biological tissues	LPE	ICP-MS	CeO <sub>2</sub> , TiO <sub>2</sub> , and CuO	ChCl: Gly (1:2), ChCl: glucose (2:1)	–/40 °C	–	–	–	–	–	–	Leaves and root of radish	–	192
Biological tissues	Microwave-assisted digestion	ICP-OES	Cu, Fe, Ni and Zn	ChCl: oxalic acid (1:2)	–/150 °C	–	0.080, 0.560, 0.040, 0.230 µg g <sup>-1</sup>	–	–	0.2–6.1%	–	Fish muscle and liver; macroalgae	>96.1%	188
Biological tissues	DES modified cotton-SPE	FAAS	Cu, Ni	ChCl: urea (1:2)	6.0/–	–	0.050, 0.600 µg L <sup>-1</sup>	–	200	4.5%, 6.8%	0.25–50.0, 4.00–12.5 µg L <sup>-1</sup>	Water and biological samples	>95.0%	194
Biological tissues	UA-extraction	FAAS	Fe	ChCl: lactic acid (1:1)	–	–	0.026 µg mL <sup>-1</sup>	0.085 µg mL <sup>-1</sup>	–	1.4%	–	Sheep, bovine and chicken liver	>95.0%	178
Biological tissues	DESS-based digestion	FAAS	Fe, Zn, and Cu	ChCl: oxalic acid (1:2)	–/100 °C	–	0.053, 0.012 and 0.006 µg g <sup>-1</sup>	5.30, 1.12, 0.63 µg g <sup>-1</sup>	–	–	0.20–4.00, 0.20–4.00, 0.10–2.00 µg mL <sup>-1</sup>	Muscle liver, gills	>95.3%	197
Biological tissues	Vortex assisted dispersive LPME	GFAAS	Hg (organic & inorganic)	[DMIM][Cl]: 1-undecanol (1:2)	1.0–3.0/50 °C	Diethyl-dithiophosphoric acid (DDTP)	0.100 µg L <sup>-1</sup>	–	112	3.7%	0.30–60.0 µg L <sup>-1</sup>	Blood sample	90.0–109.0%	198
Biological tissues	Vortex assisted dispersive LPME	ICP-MS/MS	Mn, Co, Zn, Mo	ChCl: citric acid (1:1); β-alanine: citric acid (1:1)	–/40 °C	–	0.500–1.200 µg kg <sup>-1</sup>	1.70–4.00 µg kg <sup>-1</sup>	–	0.52–2.36%	0.50–100 µg L <sup>-1</sup>	Powder barley grass	80.0–95.0%	193
Cosmetics	UA-microextraction method	FAAS	Cd, Pb	ZnCl <sub>2</sub> : acetamide (1:2)	6.0/30 °C	–	0.860, 0.660 µg L <sup>-1</sup>	–	72.5	<5%	10.0–100, 1.00–10.0 µg L <sup>-1</sup>	Lipsticks and eye shadows	>97.0%	189
Food	UA-LPME	FAAS	Cd, As	Triocylmethylammonium chloride: m-lactic acid (1:3)	7.0/–	–	0.080, 0.300 µg L <sup>-1</sup>	0.25, 1.00 µg L <sup>-1</sup>	–	2.9–4.5%	0.50–8.00, 2.00–50.0 µg L <sup>-1</sup>	Wine	90.6–103.6%	126
Food	LPME	ETAAS	Cr	ChCl: EG (1:3)	6.0/–	0.125% (w/v) azadipyrromethene dye	4.300 ng L <sup>-1</sup>	14.20 ng L <sup>-1</sup>	50	3.5%	–	Fish, mushroom samples	>95.0%	190
Food	UA-LPME	FAAS	Cu, Cd, Pb	Citric acid: sucrose (3:2)	5.5/–3.5 °C	80 µM L <sup>-1</sup> MeG <sup>2+</sup>	0.230–0.870 µg kg <sup>-1</sup>	0.78–2.94 µg kg <sup>-1</sup>	75	2.0–5.2%	0.90–1050, 1.50–675, 3.00–1200 µg kg <sup>-1</sup>	Honey	90.3–98.4%	158
Food	LLE	ICP-OES	Mn	ChCl: oxalic acid (1:1)	–/95 °C	–	0.340 µg L <sup>-1</sup>	1.13 µg L <sup>-1</sup>	–	–	10.0–3000 µg L <sup>-1</sup>	Vegetable samples	>97.0%	199
Food	LPME	MS-FAAS	Ni (ii)	Tetra butyl ammonium chloride: decanoic acid (1:3)	3.0/–	0.15% (w/v) of sodium diethyldithiocarbamate	0.130 µg L <sup>-1</sup>	0.43 µg L <sup>-1</sup>	60	3.2%	0.50–5.00 mg L <sup>-1</sup>	Onion, parsley, cigarette	91.0–99.0%	177
Food	UA-LPME	FAAS	Ni, Co	Di-Menthol: decanoic acid (1:1)	6.0/–	0.01 M 5-Br-PADAP solution	0.300/0.400 µg L <sup>-1</sup>	1.10/1.30 µg L <sup>-1</sup>	50	2.3/2.5%	1.00–130/2.00–150 µg L <sup>-1</sup>	Broccoli, spinach	95.2–102.0%	191
Food	Vortex assisted DES based LPME	FAAS	Pb	ChCl: phenol (1:2)	–	0.10% (w/v) dithizone in ethanol	8.700 µg L <sup>-1</sup>	29.00 µg L <sup>-1</sup>	–	3.1%	50.0–1000 µg L <sup>-1</sup>	Milk samples	102.5–103.2%	200
Real water	GO-HF-SPME	FAAS	Ag	ChCl: thiourea <sup>a</sup> (1:2)	4.0	–	0.200 µg L <sup>-1</sup>	0.70 µg L <sup>-1</sup>	200	3.5%	1.0–40.0 µg L <sup>-1</sup>	Tap water, spring water, river water, wastewater	>95.0%	22
Real water	UA-LPME	GF-AAS	Cr	ZnCl <sub>2</sub> : acetamide (1:3)	8–10/–	5.0 × 10 <sup>-5</sup> M calmagite	6.000 ng L <sup>-1</sup>	19.00 ng L <sup>-1</sup>	85.1	4.93%	0.012–0.300 µg L <sup>-1</sup>	Wastewater, ground water, seawater, canal water, mineralwater, tap water	>95.0%	179



Table 4 (Contd.)

Sample category	Separation & preconcentration method	Detection technique	Metal	DESS (HBA+HBD, molar ratio)	pH/Temp	Complexing agent	LOD	LOQ	PF/EF	RSD, %	Linear range	Sample details	Recoveries	Ref.
Real water	DES-LPME	ETAAS	Cr	ChCl: EG (1 : 3)	6.0/—	0.125% (w/v) azadipyrromethene dye	4.300 ng L <sup>-1</sup>	14.20 ng L <sup>-1</sup>	50	3.5%	0.200–10.0 µg L <sup>-1</sup>	Bottled mineral water, tap water, seawater, wastewater	>95.0%	190
Real water	DES-LPME	MS-FAAS	Ni	Tetra butyl ammonium chloride : decanoic acid (1 : 3)	3.0/—	0.15% (w/v) sodium diethyldithiocarbamate	0.130 µg L <sup>-1</sup>	0.43 µg L <sup>-1</sup>	60	3.2%	0.500–5.00 mg L <sup>-1</sup>	Wastewater, seawater, mineral water and well water	91.0–99.0%	177
Real water	DES-UA-LPME	FAAS	Ni and Co	<i>n</i> -Menthhol : decanoic acid (1 : 1)	6.0/—	0.01 M 5-Br-PADAP solution	0.300/0.400 µg L <sup>-1</sup>	1.10/1.30 µg L <sup>-1</sup>	50	2.3/2.5%	1.00–130/2.00–150 µg L <sup>-1</sup>	Tap water, mineral water, seawater, wastewater	95.2–102.0%	191

<sup>a</sup>Thiourea may be a carcinogen in humans since it possibly causes thyroid and liver cancers in animals.<sup>201</sup> Abbreviation: preconcentration factor (PF); enrichment/enhancement factor (EF); percentage relative standard deviation (RSD); ultrasound-assisted (UA); flame atomic absorption spectrometric determination (FAAS); graphite furnace atomic absorption spectrometry (GFAAS); liquid phase microextraction (LPME); liquid-liquid extraction (LLE); solid phase microextraction (SPME); graphene oxide reinforced inside the pores of the hollow fibre (GO-HF); choline chloride (ChCl).

(Bi<sub>2</sub>Te<sub>3</sub>), were proved to be soluble in ethaline through oxidative leaching at 45–50 °C.<sup>202</sup> The DES composed of Aliquat 336 and lactic acid was successfully applied in reverse flotation of magnetite to remove quartz in iron ore mineral samples, which increased the total Fe content of the feed ore from 53.02% to 66.80%.<sup>156</sup> In this DESs assisted reverse flotation process, Aliquat 336 acts as a collector in the synthetic agent, while lactic acid acts as a depressant. Lactic acid enables a small amount of Aliquat 336 to exist on the surface of magnetite only in the form of co-adsorption by occupying the Fe active site, which cannot improve the hydrophobicity of magnetite. Hence, quartz is brought into the float fraction to realize the reverse flotation of magnetite.<sup>156</sup> Besides, the highly efficient metal extraction capability of the DESs was also utilized in the field of soil remediation to remove heavy metals like Pb from the cataminated soil.<sup>85,203</sup>

Due to the widespread application of LIBs in the last decades, global lithium consumption has increased dramatically and is projected to reach approximately 95 000 tons in 2025,<sup>204–206</sup> while the annual global lithium production for recent years is around 69 000–85 000 tons (reported by US Geological Survey). Sustainable production and mining strategy is required to ensure lithium supply security and balance the consumption and production of lithium.<sup>207</sup> To date, several studies have reported the efficient extraction of Li from ores and brines using DESs.<sup>103,128,207</sup> A beta-diketone and a neutral extractant, the two conventional extractants, were mixed to create a new family of DESs, which were studied to extract Li from a model brine.<sup>103</sup> The results showed that the synergistic DESs composed of thenoyltrifluoroacetone (HTTA) and trioctylphosphine oxide (TOPO) (2 : 1) could efficiently and selectively extract Li from an aqueous solution containing high concentrations of Na and K ions by the LLE process with a large extraction capacity of 4.4 g L<sup>-1</sup>. In addition, the optimum DES (*i.e.*, HTTA-TOPO DES) demonstrated high reusability and stability during the long-term operation. Chen *et al.* (2021)<sup>128</sup> developed a tetrabutylammonium chloride (C<sub>4444</sub>Cl):oleic acid DES-based Li recovery system from the mother liquor with a high Na/Li ratio (>50) obtained during the production of Li<sub>2</sub>CO<sub>3</sub> (see flow diagram shown in Fig. 14). Based on the cation exchange and coordination mechanism, this recovery process exhibited better performance under alkaline conditions (pH > 10) with a high separation factor of Li/Na of 20.5 and a high extraction efficiency of above 60% even after five cycles.

#### 5.4 E-waste

The common hydrometallurgical recovery of metals from e-waste can be summarized as three main stages: pre-treatment of the raw materials, leaching and separation of metal ions, and refining of products to the desired forms (pure metal or pure metal compounds, which can be achieved by precipitation, solvent extraction, electro-deposition, *etc.*).<sup>208</sup> Due to the poor solubility and refractory (*i.e.*, it is hard to destroy the chemical structure of some of the constituents) of these metals, leaching them from natural deposits often

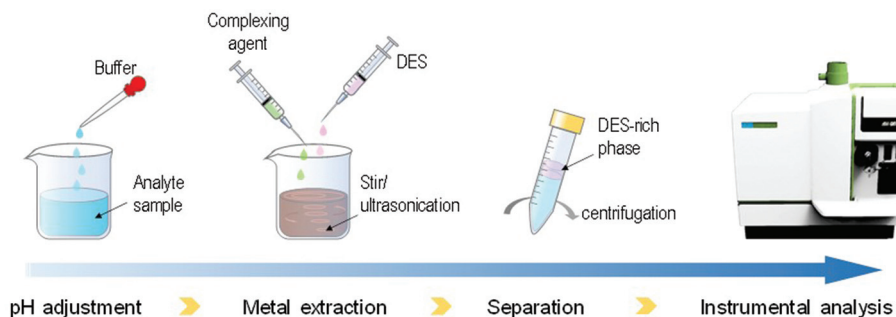


Fig. 13 Schematic procedure of commonly studied DES-based liquid phase metal extraction (LPME method).



Fig. 14 Flow diagram of the TBAC : oleic acid DES-based system from Li recovery process from the mother liquor obtained during the production of  $\text{Li}_2\text{CO}_3$ . Reprint with permission from ref. 128, Copyright © 2021, Elsevier B.V.

requires strong inorganic acids (e.g.,  $\text{HCl}$ ,  $\text{HNO}_3$ , or  $\text{H}_2\text{SO}_4$ ),<sup>209,210</sup> leading to environmental concerns. The use of DESs as green solvents provides an efficient and environmentally benign route for recycling valuable metals from e-waste.

Taking spent batteries as a practical case for the recovery of metals, Pb in spent Pb-acid batteries could be dissolved into ethaline and further recovered as metallic Pb through electro-deposition.<sup>211</sup> Co and Li from spent LIBs could be also extracted by ethaline with high extraction efficiencies (>90% for Co and >85% for Li).<sup>98,123</sup> On the other hand, reline exhibited the best performance in terms of extraction efficiencies (83.6% for Ni and 53.3% for Co) compared to other two ChCl-based DESs (ethaline and glyceline) for recovery and electrochemical formation of Ni–Co alloy from the spent Ni–metal hydride batteries.<sup>176</sup> However, it should be noted that the operating temperature and time used in these studies were significantly high and long, such as 220 °C and 24 h in the study reported by Tran *et al.* (2019),<sup>98</sup> which may not be attractive for commercial applications and hence further improvements should be sought after. Wang *et al.* (2020)<sup>154</sup> reported that the temperature and time for the extraction of Li and Co from spent LIBs could be reduced to 180 °C and 12 h by changing ethaline to reline. The use of urea as HBD in the DES helped achieve a high Li and Co extraction efficiency of over 95%, and the cubic cobalt oxide spinel ( $\text{Co}_3\text{O}_4$ ) could be obtained from the metal-loaded DES by the dilution–precipitation–calcination procedure. Roldán-Ruiz *et al.* (2020)<sup>97</sup> employed PTSA-based DES and further reduced the extraction time and temperature of Co and Li from spent batteries to 90 °C and 15 min.

Lukomska *et al.* (2021) recently compared the performance of metal recovery from “black mass”, the secondary waste from spent zinc batteries or spent LIBs, by solvent extraction technique with ILs, DESs and organophosphorus-based acids.<sup>35,36</sup> The advantages of DESs over the conventional organic solvents are lower cost, less corrosive effects on the equipment, as well as more environmentally friendly. It is because DESs inherits the features of ILs of low vapor pressure and difficult volatilization, and those based on ChCl are described as biocompatible. Meanwhile, it showed that quick (~30 min of extraction time) and efficient (over 90% extraction efficiency) recovery of Zn, Mn, Li, Co and Ni from spent batteries could be obtained using different DESs at only 318 K (~45 °C). Specifically, high recovery of metals could be achieved with ChCl:lactic acid (1 : 2) and ChCl:malnoic acid (1 : 1) DESs for extraction of Zn (~100%) and Mn (~100%)<sup>36</sup> and with ChCl:phenylacetic acid (1 : 2) DES for extraction of Co (98.7%) and Li (~100%), as well as with benzethonium chloride : lactic acid (1 : 1) for extraction of Li (~100%).<sup>35</sup> It is noteworthy that the addition of didecylmethylammonium chloride (DDACl) surfactant could increase the extraction efficiency in most metal recovery experiments using DESs, further indicating that the formation of  $[\text{MeCl}_x]^{(n-)}$  or  $[\text{MeOCl}_x]^{(n-)}$  anionic complexes should be an important step for metal extraction by type III DESs.<sup>35,36</sup>

In addition, with the assistance of microwave, the oxaline could efficiently recycle both Li and Mn ions from spent LIBs with a high extraction efficiency of 96% at only 75 °C with a leaching time of 15 min.<sup>212</sup> Additionally, Schiavi *et al.* (2021)<sup>213</sup> focused on improving the selectivity of the DESs-based solvent extraction process towards the target metals (Co, Mn) over the impurities (Fe, Al and Cu). They developed a novel solvometallurgical process containing two successive DES leaching stages conducted at different temperatures (as shown in the flow diagram in Fig. 15), which relied on the different variations in solubility of different metals in DESs. In this new process, Cu was first exclusively extracted by leaching with DES at 90 °C, while Co and Mn were dissolved in a successive leaching stage by increasing the DES temperature to 160 °C. They also found that the residual DES solution could be effectively reused in a new leaching stage, and the recovered Co could be employed to synthesize cathodic material with electrochemical performances equal to those attained with commercially available ones.





Fig. 15 Flow diagram of the solvometallurgical recycling route using ethaline. Reprint with permission from ref. 213, Copyright © 2021, Elsevier B.V.

Furthermore, green leaching processes using DESs were approached to selective extraction of various metal ions from other e-waste, including end-of-life permanent magnets,<sup>130,214</sup> lamp phosphor waste,<sup>215</sup> and printed circuit boards (PCB).<sup>96,118</sup> Specifically, the guanidine hydrochloride-lactic acid (GUC-LAC) combined DES was screened from nine kinds of guanidine-based DESs as the best leachant to selectively extract the rare earth elements, neodymium (Nd), from the end-of-life permanent magnets with a high separation factor (>1300) between Nd and Fe through a simple selective dissolution step followed by precipitation process with oxalic acid.<sup>130</sup> The ChCl:levulinic acid DES was demonstrated to have high extraction efficiency (>70%) to the red phosphor  $Y_2O_3:Eu^{3+}$  (YOX), and thus could be used as a more cost-effective alternative to IL for the selective leaching of rare earth elements (*i.e.*, yttrium (Y) and europium (Eu)) from lamp phosphor waste.<sup>215</sup> The integrated process of ultrasonic-assisted leaching in ethaline and subsequent electrodeposition showed good performance in terms of high selectivity and extraction efficiency for Sn, Pb, Zn and Cu ions from PCB.<sup>96,118</sup>

### 5.5 Industrial waste

Other than e-waste, a variety of industrial residues are also generated with the rapid development of industrialization, such as fly ash, metal finishing industry waste, spent catalyst, and wastewater. These major industrial wastes mostly contain metal elements such as Au, Ag, Zn, Cu, Pt, Pb, In, Sn, and Cu.<sup>117,151</sup> DESs have been also introduced as green solvents for metal recovery from industrial wastes. Precious metals, Au, Ag and Pd, from industrial waste could be extracted with ethaline, and Au was subsequently recovered by electro-deposition.<sup>117</sup> Zn from zinc oxide dust could dissolve in a ternary ChCl:urea:EG DES, reaching a Zn extraction efficiency of 85.2% with the slurry concentration at  $50 \text{ g L}^{-1}$ , leaching temperature at  $80 \text{ }^\circ\text{C}$ , and stir-

ring speed at 600 rpm. The pure Zn deposit was obtained through subsequent electro-deposition.<sup>5</sup> The leaching behavior of three ChCl-based DESs to selectively separate In and Sn from Zn in flue dust (mainly  $ZnFe_2O_4$ ,  $PbSO_4$  and  $Zn_2(SiO_4)$ ), and the highest leaching yields were observed in the oxalic acid system. A two-step precipitation procedure was developed to separate the target metals (In and Sn) from the main flue dust components (Fe, Zn, Pb and Cu).<sup>161</sup> Ethaline DES (ChCl:ethylene glycol with a molar ratio of 1:2) and lactiline DES (ChCl:lactic acid with a molar ratio of 1:2) were used to purify and recycle a mimicked jarosite waste stream containing Fe(III), Pb(II) and Zn(II), and the former DES exhibited better selectivity.<sup>216</sup> A process integrating DES-based LLE and precipitation to separate Fe(III), Pb(II) and Zn(II), respectively, from the jarosite wastewater, was developed and shown in Fig. 16.

The DESs-based process for metal recovery from industrial waste has been validated in pilot-scale study for Zn and Pb recovery from a waste material produced by the electric arc furnace.<sup>217</sup> An image and schematic diagram of the pilot plant are shown in Fig. 17. In this study, again a ternary DES ChCl:EG:urea (1:1.5:0.5) was used, which showed relatively low viscosity ( $\sim 56 \text{ cP}$  at  $298 \text{ K}$ ) and was effective for separation. A high selectivity towards ZnO and PbO from the electric arc furnace dust was observed with respect to FeO and  $Al_2O_3$ . It should be highlighted that the performance of the DESs for metal recovery improved when it was scaled up to pilot plant because of the better mixing conditions in the larger tank and the further lower viscosity of the DESs as the particles break up the solvent structure and aid mass transport. Pb could be further cemented by the addition of Zn dust since the former is not economically worth extracting due to its relatively low price. Zn was subsequently recovered as  $ZnCl_2$  through precipitation with the addition of ammonia, which was more economically efficient than electrodeposition.<sup>217</sup>





Fig. 16 Proposed flowsheet for the separation and recovery of Fe(III), Pb(II) and Zn(II) from a mimicked jarosite waste stream. Reprint with permission from ref. 216, Copyright © 2020, Royal Society of Chemistry.

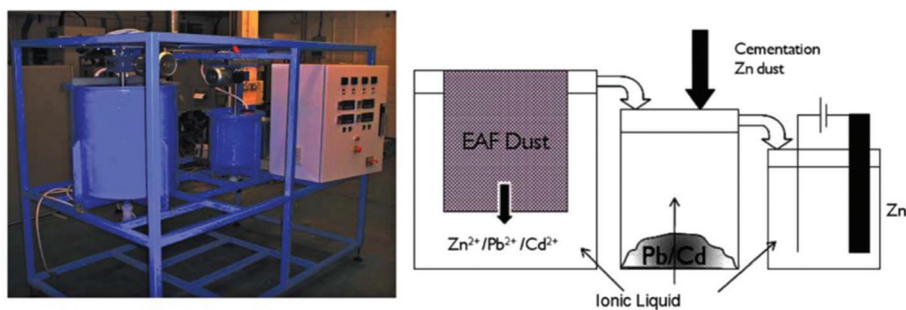


Fig. 17 Photograph and schematic diagram of the pilot scale studies to recover Zn and Pb from electric arc furnace dust by DES. Reprint with permission from ref. 217, Copyright © 2011, Royal Society of Chemistry.

## 6. Conclusions and perspectives

DESs are environmentally friendly solvents featuring highly tunable physicochemical properties, low cost, nontoxicity and biodegradability. Given such exceptional advantages coupled with the ease of preparation and good thermal and chemical stability, DESs have attracted increasing interest in recent years and shown promising results in a variety of applications, including chemical reactions, separation processes, biotechnology and biorefinery, as well as the development of advanced materials. This review focuses on the research endeavors in metal recovery by DESs from various sources, with a special focus on the mechanisms, general hybrid processes, influencing factors and the recent advancements in applications of metal extraction by DESs.

Regarding the mechanisms of metal extraction by DESs, the high solubility of the metal oxides in DESs is contributed by the formation of the complexations between the metal ions

and the components in the DESs (*e.g.*, solvents anions, ligands), and the speciation of the metals in solution determines their behavior and reactivity of the metal salts dissolved in DESs. Precipitation and electrodeposition are usually integrated with DES-based extraction processes for metal recovery. In DES-based metal extraction integrated with precipitation, metals are first dissolved in DESs, followed by selective recovery through a multi-step precipitation sequence. On the other hand, the DES extraction integrated electro-deposition process utilized the DESs features of both selective metal dissolution and high conductivity, which showed advantages of high purity deposits, easy operation and low cost.

Physicochemical properties of the DESs, such as density, viscosity, conductivity, hydrophilicity/hydrophobicity and acidity, are key factors influencing the application scenarios, process design, and performance of the DESs-based metal extraction processes. DESs are composed of hydrogen bond donors (HBD) and hydrogen bond acceptors (HBA) in different



molar ratios, which confer them the possibility to be tunable to specific purposes and for metal recovery from different matrices. Furthermore, optimization of the extraction conditions, such as temperature will affect physicochemical properties, and pH could further improve the performance of the metal extraction by DESs.

The studies of metal extraction by DESs performed in model systems, consisting of feeds of solutions only containing the target metal salts, exhibited high extraction efficiency and selectivity to various metals, demonstrating their great application potentials. Accordingly, DESs have been investigated in metal detection and recovery from environmental samples, biological tissues, food, minerals and waste (e-waste and other industrial waste). The available studies on the practical applications were generally optimistic about this new type of green solvents and showed that DESs are promising alternatives to conventional organic solvents and ILs for metal extraction due to their favorable environmental, health and safety profiles together with their relatively low preparation cost.

Despite the significant progress that has been made in the DES-based metal extraction processes, some related subjects are still critical for further research and should be priorities before their industrial applications. First, physicochemical characterization of DESs is still underway, particularly for newly developed families like H(D)ESs or THEDESs. In addition, since the comprehensive models for predicting the properties and metal selectivity of DESs are still scarce in this field, the inevitable screening step for suitable DESs in the current studies for various metal extraction scenarios was usually time-consuming and inefficient. The COSMO-RS model has been used for the separation of non-metallic components. To optimize metal recovery and separation processes, the development of similar tools and the use of thermodynamic software (e.g., MEDUSA or PHREEQC) that can predict the properties of DESs and provide theoretical information on the behavior between metals and DESs would be highly desirable in future research.

Other than the aforementioned application, the DES-based metal extraction process can be explored for advanced implementation in other fields, including metal recovery from the spent catalysts,<sup>7</sup> remediation of the heavy metal-contaminated soil,<sup>21,8</sup> residues from low-grade ores or metal processing,<sup>7</sup> etc. Further investigations of the solubilities and behaviors of the insoluble metal-containing compounds in DESs can be interesting and favorable for extending the applications of DESs for metal recovery and separation. However, the scalable applications of the DESs for metal extraction from minerals and waste (especially the vast amount of e-waste), whilst very desirable, still lack successful reports. Thus, the pilot-scale studies and systematic techno-economic assessment as well as life cycle assessment (LCA) of the new DESs-based metal extraction process are needed to validate their application potentials.

Long term stability and reusability tests should be conducted to provide a better understanding of the robustness of DESs for separation applications. Overall, substantial progress

has been made in the research on DESs applied in the metal extraction process. Interdisciplinary collaborations between chemistry scientists and process engineers are essential for developing environmentally benign and low-cost DESs-based processes towards successful practical applications in metal extraction.

## Conflicts of interest

There are no conflicts of interest to declare.

## Acknowledgements

The University of Manchester is gratefully acknowledged for the financial support. This research was supported by the Ministry of Education, Singapore, under the Academic Research Fund Tier 1 (RG84/19). In addition, JE, QS and WFY want to thank the Green Talents program, sponsored by the German Federal Ministry of Education and Research (BMBF), for their award in 2016, which has led to and will continue to lead to fruitful collaborations.

## Notes and references

- 1 London Metal Exchange price index. Retrieved from lme.com on June 15th, 2021.
- 2 G. Chen, L. Tan, M. Xie, Y. Liu, Y. Lin, W. Tan and M. Huang, *J. Membr. Sci.*, 2020, **598**, 117803.
- 3 European Commission. Report on Critical Raw Materials for the EU 2017. [https://ec.europa.eu/growth/sectors/raw-materials/specific-interest/critical\\_en](https://ec.europa.eu/growth/sectors/raw-materials/specific-interest/critical_en) (accessed May 2020).
- 4 M. E. Mondejar, R. Avtar, H. L. B. Diaz, R. K. Dubey, J. Esteban, A. Gómez-Morales, B. Hallam, N. T. Mbungu, C. C. Okolo, K. A. Prasad, Q. She and S. Garcia-Segura, *Sci. Total Environ.*, 2021, **794**, 148539.
- 5 X.-l. Zhu, C.-y. Xu, J. Tang, Y.-x. Hua, Q.-b. Zhang, H. Liu, X. Wang and M.-t. Huang, *Trans. Nonferrous Met. Soc. China*, 2019, **29**, 2222–2228.
- 6 M. N. Le and M. S. Lee, *Miner. Process. Extr. Metall. Rev.*, 2021, **42**, 335–354.
- 7 D. J. Garole, R. Hossain, V. J. Garole, V. Sahajwalla, J. Nerkar and D. P. Dubal, *ChemSusChem*, 2020, **13**, 3079–3100.
- 8 S. Needhidasan, M. Samuel and R. Chidambaram, *J. Environ. Health Sci. Eng.*, 2014, **12**, 36.
- 9 A. Golev, G. D. Corder and M. A. Rhamdhani, *Miner. Eng.*, 2019, **137**, 171–176.
- 10 V. Forti, C. P. Baldé, R. Kuehr and G. Bel, *The Global E-Waste Monitor 2020: Quantities, Flows, and the Circular Economy Potential*, 2020.
- 11 R. Nithya, C. Sivasankari and A. Thirunavukkarasu, *Environ. Chem. Lett.*, 2021, **19**, 1347–1368.
- 12 E. Hsu, K. Barmak, A. C. West and A.-H. A. Park, *Green Chem.*, 2019, **21**, 919–936.



- 13 I. M. S. K. Ilankoon, Y. Ghorbani, M. N. Chong, G. Herath, T. Moyo and J. Petersen, *Waste Manage.*, 2018, **82**, 258–275.
- 14 A. Islam, T. Ahmed, M. R. Awual, A. Rahman, M. Sultana, A. Abd Aziz, M. U. Monir, S. H. Teo and M. Hasan, *J. Cleaner Prod.*, 2020, **244**, 118815.
- 15 J. Hao, Y. Wang, Y. Wu and F. Guo, *Resour., Conserv. Recycl.*, 2020, **157**, 104787.
- 16 M. Baniyasi, F. Vakilchah, N. Bahaloo-Horeh, S. M. Mousavi and S. Farnaud, *J. Ind. Eng. Chem.*, 2019, **76**, 75–90.
- 17 K. K. Brar, S. Magdouli, S. Etteieb, M. Zolfaghari, H. Fathollahzadeh, L. Calugaru, S.-P. Komtchou, R. Tanabene and S. K. Brar, *J. Cleaner Prod.*, 2021, **291**, 125257.
- 18 G. Chauhan, P. R. Jadhao, K. K. Pant and K. D. P. Nigam, *J. Environ. Chem. Eng.*, 2018, **6**, 1288–1304.
- 19 S. Tamjidi and A. Ameri, *Environ. Sci. Pollut. Res.*, 2020, **27**, 31105–31119.
- 20 X. Hu, Y. Zhang, Z. Ding, T. Wang, H. Lian, Y. Sun and J. Wu, *Atmos. Environ.*, 2012, **57**, 146–152.
- 21 A. D. Monnot, W. V. Christian, M. M. Abramson and M. H. Follansbee, *Food Chem. Toxicol.*, 2015, **80**, 253–260.
- 22 S. Balarastaghi, Z. Khashaiarmanesh, P. Makhdomi, S. H. Alavizadeh, Z. S. Moghadam, K. Shirani and G. Karimi, *Toxin Rev.*, 2018, **37**, 117–122.
- 23 G. S. S. Sunder, S. Adhikari, A. Rohanifar, A. Poudel and J. R. Kirchoff, *Separations*, 2020, **7**(1), 4.
- 24 J. Esteban, A. J. Vorholt and W. Leitner, *Green Chem.*, 2020, **22**, 2097–2128.
- 25 J. B. Zimmerman, P. T. Anastas, H. C. Erythropel and W. Leitner, *Science*, 2020, **367**, 397–400.
- 26 C. Capello, U. Fischer and K. Hungerbühler, *Green Chem.*, 2007, **9**, 927–934.
- 27 D. Prat, A. Wells, J. Hayler, H. Sneddon, C. R. McElroy, S. Abou-Shehada and P. J. Dunn, *Green Chem.*, 2016, **18**, 288–296.
- 28 N. Schaeffer, H. Passos, I. Billard, N. Papaiconomou and J. A. P. Coutinho, *Crit. Rev. Environ. Sci. Technol.*, 2018, **48**, 859–922.
- 29 L. Y. Wang, Q. J. Guo and M. S. Lee, *Sep. Purif. Technol.*, 2019, **210**, 292–303.
- 30 A. P. Abbott, D. Boothby, G. Capper, D. L. Davies and R. K. Rasheed, *J. Am. Chem. Soc.*, 2004, **126**, 9142–9147.
- 31 A. P. Abbott, G. Capper, D. L. Davies, H. L. Munro, R. K. Rasheed and V. Tambyrajah, *Chem. Commun.*, 2001, 2010–2011, DOI: 10.1039/B106357J.
- 32 A. P. Abbott, G. Capper, D. L. Davies, R. K. Rasheed and V. Tambyrajah, *Chem. Commun.*, 2003, (1), 70–71.
- 33 X. Li and K. Binnemans, *Chem. Rev.*, 2021, **121**, 4506–4530.
- 34 J. Rydberg, *Solvent extraction principles and practice, revised and expanded*, CRC Press, New York, 2004.
- 35 A. Łukomska, A. Wisniewska, Z. Dabrowski, D. Kolasa, S. Luchcinska and U. Domanska, *J. Mol. Liq.*, 2021, **343**, 117694.
- 36 A. Łukomska, A. Wisniewska, Z. Dabrowski, D. Kolasa, S. Luchcinska, J. Lach, K. Wrobel and U. Domanska, *J. Mol. Liq.*, 2021, **338**, 116590.
- 37 M. González-Miquel and J. Esteban, in *Comprehensive Biotechnology*, ed. M. Moo-Young, Pergamon, Oxford, 3rd edn, 2019, pp. 790–806, DOI: 10.1016/B978-0-444-64046-8.00459-6.
- 38 L. P. Silva, M. A. R. Martins, J. H. F. Conceição, S. P. Pinho and J. A. P. Coutinho, *ACS Sustainable Chem. Eng.*, 2020, **8**, 15317–15326.
- 39 E. L. Smith, A. P. Abbott and K. S. Ryder, *Chem. Rev.*, 2014, **114**, 11060–11082.
- 40 D. O. Abranches, M. A. R. Martins, L. P. Silva, N. Schaeffer, S. P. Pinho and J. A. P. Coutinho, *Chem. Commun.*, 2019, **55**, 10253–10256.
- 41 Y. P. Mbous, M. Hayyan, A. Hayyan, W. F. Wong, M. A. Hashim and C. Y. Looi, *Biotechnol. Adv.*, 2017, **35**, 105–134.
- 42 L. I. N. Tomé, V. Baião, W. da Silva and C. M. A. Brett, *Appl. Mater. Today*, 2018, **10**, 30–50.
- 43 Y. Liu, J. B. Friesen, J. B. McAlpine, D. C. Lankin, S.-N. Chen and G. F. Pauli, *J. Nat. Prod.*, 2018, **81**, 679–690.
- 44 Y. Dai, J. van Spronsen, G.-J. Witkamp, R. Verpoorte and Y. H. Choi, *Anal. Chim. Acta*, 2013, **766**, 61–68.
- 45 Y. H. Choi, J. van Spronsen, Y. Dai, M. Verberne, F. Hollmann, I. W. C. E. Arends, G.-J. Witkamp and R. Verpoorte, *Plant Physiol.*, 2011, **156**, 1701–1705.
- 46 P. W. Stott, A. C. Williams and B. W. Barry, *J. Controlled Release*, 1998, **50**, 297–308.
- 47 D. Chauhan, G. Agrawal, S. Deshmukh, S. S. Roy and R. Priyadarshini, *RSC Adv.*, 2018, **8**, 37590–37599.
- 48 M. A. Martins, E. A. Crespo, P. V. Pontes, L. P. Silva, M. Bülow, G. J. Maximo, E. A. Batista, C. Held, S. o. P. Pinho and J. o. A. Coutinho, *ACS Sustainable Chem. Eng.*, 2018, **6**, 8836–8846.
- 49 C. Florindo, L. C. Branco and I. M. Marrucho, *ChemSusChem*, 2019, **12**, 1549–1559.
- 50 R. Cañadas, M. González-Miquel, E. J. González, I. Díaz and M. Rodríguez, *Sep. Purif. Technol.*, 2021, **254**, 117590.
- 51 A. Grobelak, A. Grosser, M. Kacprzak and T. Kamizela, *J. Environ. Manage.*, 2019, **234**, 90–96.
- 52 K. Shahbaz, F. S. Mjalli, M. A. Hashim and I. M. AlNashef, *Fluid Phase Equilib.*, 2012, **319**, 48–54.
- 53 C. D'Agostino, R. C. Harris, A. P. Abbott, L. F. Gladden and M. D. Mantle, *Phys. Chem. Chem. Phys.*, 2011, **13**, 21383–21391.
- 54 A. P. Abbott, R. C. Harris and K. S. Ryder, *J. Phys. Chem. B*, 2007, **111**, 4910–4913.
- 55 A. P. Abbott, R. C. Harris, K. S. Ryder, C. D'Agostino, L. F. Gladden and M. D. Mantle, *Green Chem.*, 2011, **13**, 82–90.
- 56 W. Guo, Y. Hou, S. Ren, S. Tian and W. Wu, *J. Chem. Eng. Data*, 2013, **58**, 866–872.
- 57 A. Hayyan, F. S. Mjalli, I. M. AlNashef, T. Al-Wahaibi, Y. M. Al-Wahaibi and M. A. Hashim, *Thermochim. Acta*, 2012, **541**, 70–75.



- 58 F. S. Mjalli, G. Vakili-Nezhaad, K. Shahbaz and I. M. AlNashef, *Thermochim. Acta*, 2014, **575**, 40–44.
- 59 A. Hayyan, F. S. Mjalli, I. M. AlNashef, Y. M. Al-Wahaibi, T. Al-Wahaibi and M. A. Hashim, *J. Mol. Liq.*, 2013, **178**, 137–141.
- 60 F. Chemat, H. Anjum, A. M. Shariff, P. Kumar and T. Murugesan, *J. Mol. Liq.*, 2016, **218**, 301–308.
- 61 D. Shah and F. S. Mjalli, *Phys. Chem. Chem. Phys.*, 2014, **16**, 23900–23907.
- 62 L. Bahadori, M. H. Chakrabarti, F. S. Mjalli, I. M. AlNashef, N. S. A. Manan and M. A. Hashim, *Electrochim. Acta*, 2013, **113**, 205–211.
- 63 M. H. Shafie, R. Yusof and C.-Y. Gan, *J. Mol. Liq.*, 2019, **288**, 111081.
- 64 K. Z. Kučan, M. Perković, K. Cmrk, D. Načinović and M. Rogošić, *ChemistrySelect*, 2018, **3**, 12582–12590.
- 65 M. Francisco, A. van den Bruinhorst and M. C. Kroon, *Green Chem.*, 2012, **14**, 2153–2157.
- 66 L. K. Savi, D. Carpiné, N. Waszczynskyj, R. H. Ribani and C. W. I. Haminiuk, *Fluid Phase Equilib.*, 2019, **488**, 40–47.
- 67 Z. Maugeri and P. Domínguez de María, *RSC Adv.*, 2012, **2**, 421–425.
- 68 D. Z. Troter, Z. B. Todorovic, D. R. Dokic-Stojanovic, B. S. Dordevic, V. M. Todorovic, S. S. Konstantinovic and V. B. Veljkovic, *J. Serb. Chem. Soc.*, 2017, **82**, 1039–1052.
- 69 A. N. El-hoshoudy, F. S. Soliman, E. M. Mansour, T. Zaki and S. M. Desouky, *J. Mol. Liq.*, 2019, **294**, 111621.
- 70 N. Rodriguez Rodriguez, L. Machiels and K. Binnemans, *ACS Sustainable Chem. Eng.*, 2019, **7**, 3940–3948.
- 71 Y. Cui, C. Li, J. Yin, S. Li, Y. Jia and M. Bao, *J. Mol. Liq.*, 2017, **236**, 338–343.
- 72 S. Ruggeri, F. Poletti, C. Zanardi, L. Pigani, B. Zanfognini, E. Corsi, N. Dossi, M. Salomäki, H. Kivelä, J. Lukkari and F. Terzi, *Electrochim. Acta*, 2019, **295**, 124–129.
- 73 I. Zahrina, K. Mulia, A. Yanuar and M. Nasikin, *J. Mol. Struct.*, 2018, **1158**, 133–138.
- 74 R. Craveiro, I. Aroso, V. Flammia, T. Carvalho, M. T. Viciosa, M. Dionísio, S. Barreiros, R. L. Reis, A. R. C. Duarte and A. Paiva, *J. Mol. Liq.*, 2016, **215**, 534–540.
- 75 L. K. Savi, M. C. G. C. Dias, D. Carpine, N. Waszczynskyj, R. H. Ribani and C. W. I. Haminiuk, *Int. J. Food Sci. Technol.*, 2019, **54**, 898–907.
- 76 A. P. Abbott, J. C. Barron, K. S. Ryder and D. Wilson, *Chem. – Eur. J.*, 2007, **13**, 6495–6501.
- 77 A. Abo-Hamad, M. Hayyan, M. A. AlSaadi and M. A. Hashim, *Chem. Eng. J.*, 2015, **273**, 551–567.
- 78 G. García, S. Aparicio, R. Ullah and M. Atilhan, *Energy Fuels*, 2015, **29**, 2616–2644.
- 79 P. Liu, J.-W. Hao, L.-P. Mo and Z.-H. Zhang, *RSC Adv.*, 2015, **5**, 48675–48704.
- 80 S. C. Cunha and J. O. Fernandes, *TrAC, Trends Anal. Chem.*, 2018, **105**, 225–239.
- 81 B. Tang and K. H. Row, *Monatsh. Chem. – Chem. Mon.*, 2013, **144**, 1427–1454.
- 82 Q. Zhang, K. De Oliveira Vigier, S. Royer and F. Jérôme, *Chem. Soc. Rev.*, 2012, **41**, 7108–7146.
- 83 H. Qin, X. Hu, J. Wang, H. Cheng, L. Chen and Z. Qi, *Green Energy Environ.*, 2020, **5**, 8–21.
- 84 P. Makoš, E. Słupek and J. Gębicki, *Microchem. J.*, 2020, **152**, 104384.
- 85 M. Zhang, X. Zhang, Y. Liu, K. Wu, Y. Zhu, H. Lu and B. Liang, *Environ. Sci. Pollut. Res.*, 2021, **28**(27), 35537–35563.
- 86 N. Schaeffer, J. H. F. Conceição, M. A. R. Martins, M. C. Neves, G. Pérez-Sánchez, J. R. B. Gomes, N. Papaiconomou and J. A. P. Coutinho, *Green Chem.*, 2020, **22**, 2810–2820.
- 87 W. Tang, Y. An and K. H. Row, *TrAC, Trends Anal. Chem.*, 2021, **136**, 116187.
- 88 A. Singh, R. Walvekar, K. Mohammad, W. Y. Wong and T. C. S. M. Gupta, *J. Mol. Liq.*, 2018, **252**, 439–444.
- 89 A. K. Jangir, P. Sethy, G. Verma, P. Bahadur and K. Kuperkar, *J. Mol. Liq.*, 2021, **332**, 115909.
- 90 E. L. Byrne, R. O'Donnell, M. Gilmore, N. Artioli, J. D. Holbrey and M. Swadźba-Kwaśny, *Phys. Chem. Chem. Phys.*, 2020, **22**, 24744–24763.
- 91 A. Entezari-Zarandi and F. Larachi, *J. Rare Earths*, 2019, **37**, 528–533.
- 92 M. K. AlOmar, M. Hayyan, M. A. Alsaadi, S. Akib, A. Hayyan and M. A. Hashim, *J. Mol. Liq.*, 2016, **215**, 98–103.
- 93 O. S. Hammond, D. T. Bowron, A. J. Jackson, T. Arnold, A. Sanchez-Fernandez, N. Tsapatsaris, V. G. Sakai and K. J. Edler, *J. Phys. Chem. B*, 2017, **121**, 7473–7483.
- 94 O. S. Hammond, D. T. Bowron and K. J. Edler, *Angew. Chem., Int. Ed.*, 2017, **56**, 9782–9785.
- 95 M. R. S. Foreman, *Cogent Chem.*, 2016, **2**, 1139289.
- 96 M.-L. Doche, A. Mandroyan, M. Mourad-Mahmoud, V. Moutarlier and J.-Y. Hihn, *Chem. Eng. Process.*, 2017, **121**, 90–96.
- 97 M. J. Roldán-Ruiz, M. L. Ferrer, M. C. Gutiérrez and F. d. Monte, *ACS Sustainable Chem. Eng.*, 2020, **8**, 5437–5445.
- 98 M. K. Tran, M.-T. F. Rodrigues, K. Kato, G. Babu and P. M. Ajayan, *Nat. Energy*, 2019, **4**, 339–345.
- 99 B. B. Hansen, S. Spittle, B. Chen, D. Poe, Y. Zhang, J. M. Klein, A. Horton, L. Adhikari, T. Zelovich, B. W. Doherty, B. Gurkan, E. J. Maginn, A. Ragauskas, M. Dadmun, T. A. Zawodzinski, G. A. Baker, M. E. Tuckerman, R. F. Savinell and J. R. Sangoro, *Chem. Rev.*, 2021, **121**, 1232–1285.
- 100 A. P. Abbott, *ChemPhysChem*, 2005, **6**, 2502–2505.
- 101 F. S. G. Bagh, K. Shahbaz, F. S. Mjalli, M. A. Hashim and I. M. AlNashef, *J. Mol. Liq.*, 2015, **204**, 76–83.
- 102 A. P. Abbott, G. Capper and S. Gray, *ChemPhysChem*, 2006, **7**, 803–806.
- 103 T. Hanada and M. Goto, *ACS Sustainable Chem. Eng.*, 2021, **9**, 2152–2160.
- 104 M. Taghizadeh, A. Taghizadeh, V. Vatanpour, M. R. Ganjali and M. R. Saeb, *Sep. Purif. Technol.*, 2021, **258**, 26.
- 105 Z. Maugeri and P. Domínguez de María, *ChemCatChem*, 2014, **6**, 1535–1537.





- 106 M. S. Rahman and D. E. Raynie, *J. Mol. Liq.*, 2021, **324**, 114779.
- 107 H. Zhao, G. A. Baker and S. Holmes, *J. Mol. Catal. B: Enzym.*, 2011, **72**, 163–167.
- 108 M. Francisco, A. van den Bruinhorst and M. C. Kroon, *Angew. Chem., Int. Ed.*, 2013, **52**, 3074–3085.
- 109 I. M. Pateli, A. P. Abbott, G. R. T. Jenkin and J. M. Hartley, *Green Chem.*, 2020, **22**, 8360–8368.
- 110 W. Chen, Z. Xue, J. Wang, J. Jiang, X. Zhao and T. Mu, *Acta Phys.-Chim. Sin.*, 2018, **34**, 904–911.
- 111 E. S. Morais, M. G. Freire, C. S. Freire, J. A. Coutinho and A. J. Silvestre, *ChemSusChem*, 2020, **13**, 784–790.
- 112 B. D. Ribeiro, C. Florindo, L. C. Iff, M. A. Coelho and I. M. Marrucho, *ACS Sustainable Chem. Eng.*, 2015, **3**, 2469–2477.
- 113 N. Schaeffer, M. A. R. Martins, C. M. S. S. Neves, S. P. Pinho and J. A. P. Coutinho, *Chem. Commun.*, 2018, **54**, 8104–8107.
- 114 Y. Geng, Z. Xiang, C. Lv, N. Wang, Y. Wang and Y. Yang, *Hydrometallurgy*, 2019, **188**, 264–271.
- 115 N. Tang, L. Liu, C. Yin, G. Zhu, Q. Huang, J. Dong, X. Yang and S. Wang, *J. Taiwan Inst. Chem. Eng.*, 2021, **121**, 92–100.
- 116 A. P. Abbott, G. Capper, D. L. Davies, K. J. McKenzie and S. U. Obi, *J. Chem. Eng. Data*, 2006, **51**, 1280–1282.
- 117 G. R. T. Jenkin, A. Z. M. Al-Bassam, R. C. Harris, A. P. Abbott, D. J. Smith, D. A. Holwell, R. J. Chapman and C. J. Stanley, *Miner. Eng.*, 2016, **87**, 18–24.
- 118 A. M. Popescu, C. Donath, E. I. Neacsu, V. Soare, I. Constantin, M. Burada, D. V. Dumitrescu, K. Yanuskevich and V. Constantin, *Rev. Chim.*, 2017, **68**, 1963–1968.
- 119 A. Bakkar and V. Neubert, *J. Alloys Compd.*, 2019, **771**, 424–432.
- 120 M. Manolova and R. Böck, *Trans. IMF*, 2019, **97**, 161–168.
- 121 F. Danilov, A. Kityk, D. Shaiderov, D. Bogdanov, S. Korniy and V. Protsenko, *Surf. Eng. Appl. Electrochem.*, 2019, **55**, 138–149.
- 122 J. A. Juma, *Arabian J. Chem.*, 2021, **14**, 103036.
- 123 H. Guo, Z. Min, Y. Hao, X. Wang, J. Fan, P. Shi, Y. Min and Q. Xu, *Sci. Total Environ.*, 2021, **759**, 143478.
- 124 J. Lee, D. Jung and K. Park, *TrAC, Trends Anal. Chem.*, 2019, **118**, 853–868.
- 125 D. J. G. P. van Osch, L. F. Zubeir, A. van den Bruinhorst, M. A. A. Rocha and M. C. Kroon, *Green Chem.*, 2015, **17**, 4518–4521.
- 126 Y. Ji, M. Zhao, A. Li and L. Zhao, *Microchem. J.*, 2021, **164**, 105974.
- 127 D. J. G. P. van Osch, D. Parmentier, C. H. J. T. Dietz, A. van den Bruinhorst, R. Tuinier and M. C. Kroon, *Chem. Commun.*, 2016, **52**, 11987–11990.
- 128 W. Chen, X. Li, L. Chen, G. Zhou, Q. Lu, Y. Huang, Y. Chao and W. Zhu, *Chem. Eng. J.*, 2021, **420**, 127648.
- 129 I. M. Pateli, D. Thompson, S. S. M. Alabdullah, A. P. Abbott, G. R. T. Jenkin and J. M. Hartley, *Green Chem.*, 2020, **22**, 5476–5486.
- 130 C. Liu, Q. Yan, X. Zhang, L. Lei and C. Xiao, *Environ. Sci. Technol.*, 2020, **54**, 10370–10379.
- 131 S. Khandelwal, Y. K. Tailor and M. Kumar, *J. Mol. Liq.*, 2016, **215**, 345–386.
- 132 J. Esteban, H. Warmeling and A. J. Vorholt, *Catal. Commun.*, 2019, **129**, 105721.
- 133 M. K. Hadj-Kali, Z. Salleh, E. Ali, R. Khan and M. A. Hashim, *Fluid Phase Equilib.*, 2017, **448**, 152–167.
- 134 A. Klamt, *J. Phys. Chem.*, 1995, **99**, 2224–2235.
- 135 A. Klamt, *COSMO-RS: From Quantum Chemistry to Fluid Phase Thermodynamics and Drug Design*, Elsevier, Amsterdam, The Netherlands, 2005.
- 136 P. López-Porfiri, P. Gorgojo and M. Gonzalez-Miquel, *ACS Sustainable Chem. Eng.*, 2020, **8**(24), 8958–8969.
- 137 S. Tahir, U. Y. Qazi, Z. Naseem, N. Tahir, M. Zahid, R. Javaid and I. Shahid, *Fuel*, 2021, **305**, 121502.
- 138 M. H. Zainal-Abidin, M. Hayyan, A. Hayyan and N. S. Jayakumar, *Anal. Chim. Acta*, 2017, **979**, 1–23.
- 139 Y. Zhang, X. Ji and X. Lu, *Renewable Sustainable Energy Rev.*, 2018, **97**, 436–455.
- 140 H. Zhao and G. A. Baker, *J. Chem. Technol. Biotechnol.*, 2013, **88**, 3–12.
- 141 D. Z. Troter, Z. B. Todorović, D. R. Đokić-Stojanović, O. S. Stamenković and V. B. Veljković, *Renewable Sustainable Energy Rev.*, 2016, **61**, 473–500.
- 142 Y. T. Tan, A. S. M. Chua and G. C. Nghoh, *Bioresour. Technol.*, 2020, **297**, 122522.
- 143 W. Wang and D.-J. Lee, *Bioresour. Technol.*, 2021, **339**, 125587.
- 144 M. Pätzold, S. Siebenhaller, S. Kara, A. Liese, C. Syldatk and D. Holtmann, *Trends Biotechnol.*, 2019, **37**, 943–959.
- 145 V. Gotor-Fernández and C. E. Paul, *J. Biotechnol.*, 2019, **293**, 24–35.
- 146 J. Cao and E. Su, *J. Cleaner Prod.*, 2021, **314**, 127965.
- 147 A. E. Ünlü, A. Arıkaya and S. Takaç, *Green Process. Synth.*, 2019, **8**(1), 355–372.
- 148 J. M. Hartley, C.-M. Ip, G. C. Forrest, K. Singh, S. J. Gurman, K. S. Ryder, A. P. Abbott and G. Frisch, *Inorg. Chem.*, 2014, **53**, 6280–6288.
- 149 X. Shen, N. Sinclair, J. Wainright, R. Akolkar and R. F. Savinell, *J. Electrochem. Soc.*, 2020, **167**(8), 086509.
- 150 C. D'Agostino, L. F. Gladden, M. D. Mantle, A. P. Abbott, E. I. Ahmed, A. Y. M. Al-Murshedi and R. C. Harris, *Phys. Chem. Chem. Phys.*, 2015, **17**, 15297–15304.
- 151 G. Damilano, A. Laitinen, P. Willberg-Keyriläinen, T. Lavonen, R. Häkkinen, W. Dehaen, K. Binnemans and L. Kuutti, *RSC Adv.*, 2020, **10**, 23484–23490.
- 152 A. Tessier, P. G. Campbell and M. Bisson, *Anal. Chem.*, 1979, **51**, 844–851.
- 153 D. W. Shoesmith, J. Tait, S. Sunder, W. Gray, S. Steward, R. Russo and J. Rudnicki, *Factors affecting the differences in reactivity and dissolution rates between UO<sub>2</sub> and spent nuclear fuel*, Atomic Energy of Canada Ltd., 1996.
- 154 S. Wang, Z. Zhang, Z. Lu and Z. Xu, *Green Chem.*, 2020, **22**, 4473–4482.



- 155 N. Peeters, K. Binnemans and S. Riaño, *Green Chem.*, 2020, **22**, 4210–4221.
- 156 C. Liu, G. Mei, M. Yu, Q. Cheng and S. Yang, *Chem. Phys. Lett.*, 2021, **762**, 138152.
- 157 H. U. Haq, M. Balal, R. Castro-Muñoz, Z. Hussain, F. Safi, S. Ullah and G. Boczkaj, *J. Mol. Liq.*, 2021, **333**, 115930.
- 158 N. Altunay, A. Elik and R. Gürkan, *Microchem. J.*, 2019, **147**, 49–59.
- 159 R. Liu, Y. Geng, Z. Tian, N. Wang, M. Wang, G. Zhang and Y. Yang, *Hydrometallurgy*, 2021, **199**, 105521.
- 160 M. Allan, L. S. Taylor and L. J. Mauer, *Food Chem.*, 2016, **195**, 2–10.
- 161 P. Zürner and G. Frisch, *ACS Sustainable Chem. Eng.*, 2019, **7**, 5300–5308.
- 162 W. Gao, J. Song, H. Cao, X. Lin, X. Zhang, X. Zheng, Y. Zhang and Z. Sun, *J. Cleaner Prod.*, 2018, **178**, 833–845.
- 163 Q. Lu, L. Chen, X. Li, Y. Chao, J. Sun, H. Ji and W. Zhu, *ACS Sustainable Chem. Eng.*, 2021, **9**, 13851–13861.
- 164 J. Ru, Y. Hua, C. Xu, J. Li, Y. Li, D. Wang, C. Qi and Y. Jie, *Appl. Surf. Sci.*, 2015, **335**, 153–159.
- 165 C. G. Poll, G. W. Nelson, D. M. Pickup, A. V. Chadwick, D. J. Riley and D. J. Payne, *Green Chem.*, 2016, **18**, 2946–2955.
- 166 P. Sebastian, M. I. Giannotti, E. Gómez and J. M. Feliu, *ACS Appl. Energy Mater.*, 2018, **1**, 1016–1028.
- 167 J. Ru, Y. Hua, D. Wang, C. Xu, Q. Zhang, J. Li and Y. Li, *Electrochim. Acta*, 2016, **196**, 56–66.
- 168 P. Cen, K. Spahiu, M. S. Tyumentsev and M. R. S. J. Foreman, *Phys. Chem. Chem. Phys.*, 2020, **22**, 11012–11024.
- 169 N. A. Milevskii, I. V. Zinov'eva, Y. A. Zakhodyaeva and A. A. Voshkin, *Hydrometallurgy*, 2022, **207**, 105777.
- 170 V. Migliorati, G. Fazio, S. Pollastri, A. Gentili, P. Tomai, F. Tavani and P. D'Angelo, *J. Mol. Liq.*, 2021, **329**, 115505.
- 171 F.-J. Albler, K. Bica, M. R. S. Foreman, S. Holgersson and M. S. Tyumentsev, *J. Cleaner Prod.*, 2017, **167**, 806–814.
- 172 M. R. S. J. Foreman, S. Holgersson, C. McPhee and M. S. Tyumentsev, *New J. Chem.*, 2018, **42**, 2006–2012.
- 173 S. J. R. Vargas, G. Pérez-Sánchez, N. Schaeffer and J. A. P. Coutinho, *Green Chem.*, 2021, **23**, 4540–4550.
- 174 M. Manolova, R. Böck, I. Scharf, T. Mehner and T. Lampke, *J. Alloys Compd.*, 2021, **855**, 157462.
- 175 A. P. Abbott, G. Capper, K. J. McKenzie and K. S. Ryder, *J. Electroanal. Chem.*, 2007, **599**, 288–294.
- 176 M. Landa-Castro, J. Aldana-González, M. G. M. de Oca-Yemha, M. Romero-Romo, E. M. Arce-Estrada and M. Palomar-Pardavé, *J. Alloys Compd.*, 2020, **830**, 154650.
- 177 Z. Erbas, M. Soylak, E. Yilmaz and M. Dogan, *Microchem. J.*, 2019, **145**, 745–750.
- 178 E. Yilmaz and M. Soylak, *Talanta*, 2015, **136**, 170–173.
- 179 J. Ali, M. Tuzen, D. Citak, O. D. Uluozlu, D. Mendil, T. G. Kazi and H. I. Afridi, *J. Mol. Liq.*, 2019, **291**, 111299.
- 180 J. A. Baig, L. Elci, M. I. Khan and T. G. Kazi, *J. AOAC Int.*, 2019, **97**, 1421–1425.
- 181 M. A. Kareem, F. S. Mjalli, M. A. Hashim and I. M. AlNashef, *J. Chem. Eng. Data*, 2010, **55**, 4632–4637.
- 182 Z. Bahadır, V. N. Bulut, D. Ozdes, C. Duran, H. Bektas and M. Soylak, *J. Ind. Eng. Chem.*, 2014, **20**, 1030–1034.
- 183 I. Rykowska, J. Ziemblińska and I. Nowak, *J. Mol. Liq.*, 2018, **259**, 319–339.
- 184 H. Peng, N. Zhang, M. He, B. Chen and B. Hu, *Talanta*, 2015, **131**, 266–272.
- 185 L. Xie, S. Liu, Z. Han, R. Jiang, H. Liu, F. Zhu, F. Zeng, C. Su and G. Ouyang, *Anal. Chim. Acta*, 2015, **853**, 303–310.
- 186 X. Wang, L. Shi, Q. Lin, X. Zhu and Y. Duan, *J. Anal. At. Spectrom.*, 2014, **29**, 1098–1104.
- 187 D. Bakircioglu, Y. B. Kurtulus and G. Ucar, *Food Chem. Toxicol.*, 2011, **49**, 202–207.
- 188 K. Ghanemi, M.-A. Navidi, M. Fallah-Mehrjardi and A. Dadolahi-Sohrab, *Anal. Methods*, 2014, **6**, 1774–1781.
- 189 T. G. Kazi, H. I. Afridi, M. Bhatti and A. Akhtar, *Ultrason. Sonochem.*, 2019, **51**, 40–48.
- 190 A. H. Panhwar, M. Tuzen, N. Deligonul and T. G. Kazi, *Appl. Organomet. Chem.*, 2018, **32**, e4319.
- 191 M. Tavakoli, M. R. Jamali and A. Nezhadali, *Anal. Lett.*, 2021, 1–12, DOI: 10.1080/00032719.2021.1897990.
- 192 M. Jakubowska and L. Ruzik, *Anal. Biochem.*, 2021, **617**, 114117.
- 193 N. Osowska, K. Paduszyński, M. Matczuk and L. Ruzik, *J. Anal. At. Spectrom.*, 2021, **36**, 946–953.
- 194 M. Karimi, S. Dadfarnia and A. M. H. Shabani, *Biol. Trace Elem. Res.*, 2017, **176**, 207–215.
- 195 A. H. Panhwar, M. Tuzen and T. G. Kazi, *J. AOAC Int.*, 2018, **101**, 1183–1189.
- 196 X. Yang, Y.-Y. Zang, S. Yang and Z.-G. Chen, *J. Sci. Food Agric.*, 2021, **101**, 2930–2939.
- 197 E. Habibi, K. Ghanemi, M. Fallah-Mehrjardi and A. Dadolahi-Sohrab, *Anal. Chim. Acta*, 2013, **762**, 61–67.
- 198 R. Akramipour, M. R. Golpayegani, S. Gheini and N. Fattahi, *Talanta*, 2018, **186**, 17–23.
- 199 E. Bağda, H. Altundağ and M. Soylak, *Biol. Trace Elem. Res.*, 2017, **179**, 334–339.
- 200 T. Borahan, T. Unutkan, N. B. Turan, F. Turak and S. Bakirdere, *Food Chem.*, 2019, **299**, 125065.
- 201 S. C. Mitchell and G. B. Steventon, *Sulfur Rep.*, 1994, **16**, 117–137.
- 202 G. R. Jenkin, A. Z. Al-Bassam, R. C. Harris, A. P. Abbott, D. J. Smith, D. A. Holwell, R. J. Chapman and C. J. Stanley, *Miner. Eng.*, 2016, **87**, 18–24.
- 203 S. Mukhopadhyay, S. Mukherjee, N. F. Adnan, A. Hayyan, M. Hayyan, M. A. Hashim and B. Sen Gupta, *Chem. Eng. J.*, 2016, **294**, 316–322.
- 204 X. Xu, Y. Chen, P. Wan, K. Gasem, K. Wang, T. He, H. Adidharma and M. Fan, *Prog. Mater. Sci.*, 2016, **84**, 276–313.
- 205 X. Li, Y. Mo, W. Qing, S. Shao, C. Y. Tang and J. Li, *J. Membr. Sci.*, 2019, **591**, 117317.
- 206 A. Zhao, J. Liu, X. Ai, H. Yang and Y. Cao, *ChemSusChem*, 2019, **12**, 1361–1367.
- 207 A. Masmoudi, G. Zante, D. Trébouet, R. Barillon and M. Boltoeva, *Sep. Purif. Technol.*, 2021, **255**, 117653.



- 208 C. Tunsu, M. Petranikova, M. Gergorić, C. Ekberg and T. Retegan, *Hydrometallurgy*, 2015, **156**, 239–258.
- 209 J. Yang, C. Ekberg and T. Retegan, *Int. J. Chem. Eng.*, 2014, **2014**, 186768.
- 210 J. Yang, T. Retegan and C. Ekberg, *Hydrometallurgy*, 2013, **137**, 68–77.
- 211 A. D. Ballantyne, J. P. Hallett, D. J. Riley, N. Shah and D. J. Payne, *R. Soc. Open Sci.*, 2018, **5**, 171368.
- 212 Z. Xu, H. Shao, Q. Zhao and Z. Liang, *JOM*, 2021, **73**, 2104–2110.
- 213 P. G. Schiavi, P. Altimari, M. Branchi, R. Zanoni, G. Simonetti, M. A. Navarra and F. Pagnanelli, *Chem. Eng. J.*, 2021, **417**, 129249.
- 214 S. Riaño, M. Petranikova, B. Onghena, T. Vander Hoogerstraete, D. Banerjee, M. R. S. Foreman, C. Ekberg and K. Binnemans, *RSC Adv.*, 2017, **7**, 32100–32113.
- 215 I. M. Pateli, A. P. Abbott, K. Binnemans and N. Rodriguez Rodriguez, *RSC Adv.*, 2020, **10**, 28879–28890.
- 216 S. Spatharriotis, N. Peeters, K. S. Ryder, A. P. Abbott, K. Binnemans and S. Riano, *RSC Adv.*, 2020, **10**, 33161–33170.
- 217 A. P. Abbott, G. Frisch, J. Hartley and K. S. Ryder, *Green Chem.*, 2011, **13**, 471–481.
- 218 S. Sharma, S. Tiwari, A. Hasan, V. Saxena and L. M. Pandey, *3 Biotech.*, 2018, **8**, 216.

